Differential response of two common human papillomavirus 16

E6 variants to small interfering RNA

A thesis presented to

The Faculty of Graduate Studies

of

Lakehead University

by

MELISSA TOGTEMA

In partial fulfillment of requirements
for the degree of
Master of Science in Biology

August 28, 2013

ABSTRACT

High-risk human papillomaviruses (HPVs), such as HPV16, are implicated in causing virtually all cases of cervical cancer. Molecular therapies capable of targeting HPV16 E6 oncoprotein expression can selectively eliminate infected cells without the unwanted side effects in healthy cells seen with traditional treatments. An efficient approach is the use of synthetic small interfering RNA (siRNA) to target and degrade E6 mRNA. Two common variants of the HPV16 E6 gene, European Prototype (EP E6) and Asian-American (AA E6), differ due to six single nucleotide polymorphisms (SNPs) and AA E6 has been shown to have a greater oncogenic potential than EP E6. *In silico* modeling was used to demonstrate that these AA E6 SNPs cause its mRNA to have a less compacted structure than that of EP E6. However, transfection of an E6 siRNA containing no base pair mismatches with either variant demonstrated that these structural changes did not result in AA E6 having a significantly different amount of E6 knockdown than EP E6, as determined using RT-qPCR. Interestingly, equivalent knockdown of E6 mRNA in both variants yielded differing responses in the restoration of downstream cellular process abrogated by E6. hTERT mRNA levels were equally restored to those of PHFKs in AA E6. There was a greater elevation of IFN β mRNA expression in EP compared to AA E6. AA E6 IFN κ mRNA and p53 protein levels were elevated more following treatment with a lower dose of E6 siRNA than those of EP E6. These data add to the growing body of evidence that the AA E6 protein may have unique properties or disrupt cellular processes through different mechanisms compared to EP E6. These findings also have translational implications (e.g. different doses of E6 siRNA may be required to achieve the same therapeutic effect, depending on the variant involved).

LAY SUMMARY

Faculty and students in the Department of Biology are bound together by a common interest in explaining the diversity of life, the fit between form and function, and the distribution and abundance of organisms. Human papillomavirus 16 (HPV16) is a sexually transmitted virus, which is linked to causing almost all cases of cervical cancer. Two naturally occurring, common variants of HPV16 E6, the main cancer causing protein produced by the virus, are European Prototype and Asian-American. This study focused on determining whether a therapeutic molecule that specifically targets the expression of the E6 protein would work equally as well against both variants. In addition, it was investigated whether cellular processes altered by the HPV16 E6 protein, such as the ability to launch an immune response against invading pathogens, were equally restored in both variants following treatment with this therapeutic molecule. This information helps us better understand how these two variants function differently and gives us useful knowledge about how to better treat HPV16 infections depending on which variant the patient is infected with.

DEDICATION

To my Mom and Dad for never letting me give up on my dreams.

ACKNOWLEDGEMENTS

Professional

First and foremost, thank you to my supervisor and mentor, Dr. Ingeborg Zehbe for seeing the potential in me. The many hours you have spent teaching me the wet lab "tricks of the trade" and discussing the ever-changing status of our projects were very much appreciated. I cannot express enough gratitude for all the opportunities you have given me to grow as a student, a budding scientist, and a lab manager during my time at the Thunder Bay Regional Research Institute (TBRRI). I have an all new level of respect for how challenging it is to become a successful researcher!

To my committee members, Dr. Heidi Schraft and Dr. Wensheng Qin, thank you for the guidance and many helpful suggestions. As well, thank you to my external reviewer, Dr. Andreas Kaufmann, from the Department of Gynaecological Tumour Immunology at the Charité in Berlin, Germany, for taking the time to evaluate my thesis.

Dr. Wely Floriano, I am very grateful for all of your help developing the *in silico* structural models for the E6 variant mRNAs. I appreciate your time and patience while going over the methods and results. A special thank you to Dr. Jyoti Chattopadhyaya, from the Department of Cell and Molecular Biology at Uppsala Univeristy, Sweden, for the many thought (and experiment!) provoking conversations about siRNA therapeutics and chemical modifications. Thanks to Dr. David Law for very kindly letting me borrow the use of your lab for Experion analysis.

And of course, thank you to all of the scientists and my colleagues at the TBRRI for making it such a great academic environment to work in. To my lab mates and friends Rob and Sean, I would have been lost without you guys! Rob, all the time you took out of

your busy schedule to help me wrangle biostatistics, R, and just about every other computer program out there as well as to lend an ear to all my questions certainly did not go unappreciated. Sean (Kevin Bacon), without your awesome lab skills, I never would have mastered the elusive HA Western blot. You both were great at knowing when to give me a push to keep going or when to call it a day and get some coffee. Also, thanks to the undergraduate students I had the great opportunity to mentor, Jasmine and Greg. Your unique perspectives on my experiments helped me conquer several hurdles.

Personal

My family and friends, thanks for being patient and understanding during the times when I was so busy that I was practically living in my lab. Your constant support kept me going! To my loving husband Greg, MSc and P. Eng., thanks for reminding me that, although it isn't always easy, an academic career is a rewarding and worthwhile venture. Your late night dinner deliveries to the lab were a lifesaver! Mom and Dad, no matter where I've gone and no matter what I've done, you've always been there to support my decisions and this was no exception! Thanks for all the love, care and encouragement and for letting me move back home for two weeks to finish writing this thesis. As always, I don't know what I would do without you!

TABLE OF CONTENTS

LIST OF TABLES

LIST OF ABBREVIATIONS

6-FAM	carboxyfluorescein
AA E6	Asian-American variant of HPV16
ANOVA	analysis of variance
APS	ammonium persulfate
bp	base pair
BSA	bovine serum albumin
CIN	cervical intraepithelial neoplasia
Ct	cycle threshold
dH_2O	distilled water
DMSO	dimethyl sulfoxide
DPBS	Dulbecco's phosphate-buffered saline
dsRNA	double-stranded RNA
EDTA	ethylenediaminetetraacetic acid
EP E6	European Prototype variant of HPV16
HA	hemagglutinin
HPRT1	hypoxanthine phosphoribosyltransferase 1
HPV	human papillomavirus
hTERT	catalytic subunit of enzyme telomerase
HRP	horseradish peroxidase
ICAM-1	intercellular adhesion molecule-1/CD54
ICTV	International Committee on Taxonomy of Viruses

IFN	interferon
LCR	long control region
LEEP	loop electrosurgical excision procedure
miRNA	micro-RNA
NIKS	Near-Diploid Immortalized Keratinocytes
NMR	nuclear magnetic resonance
nt	nucleotide
ORF	open reading frame
p53	tumour suppressor protein
PAE	early polyadenylation site
PAL	late polyadenylation site
PARP	poly(ADP-ribose) polymerase-1
Pap Test	Papanicolaou test
PCR	polymerase chain reaction
PE	early promoter
PHFK	primary human foreskin keratinocyte
PL	late promoter
PMSF	phenylmethylsulfonyl fluoride
pRb	retinoblastoma protein
RISC	RNA induced silencing complex
RNAi	RNA interference
RT-qPCR	real-time reverse transcription polymerase chain reaction
SDS	sodium dodecyl sulphate

shRNA	short-hairpin RNA
siRNA	small interfering RNA
SNP	single nucleotide polymorphism
TBE	tris/borate/EDTA buffer
TBST	tris buffered saline with 0.05% TWEEN® 20
TEMED	tetramethylethylenediamine
TLR	toll-like receptor
UTR	untranslated region

1 INTRODUCTION

1.1 Human Papillomavirus and its Association with Cancer

Human papillomaviruses (HPVs) are double-stranded DNA viruses which infect the keratinocytes of skin and mucosa (zur Hausen 2002). HPVs are divided into 5 genera: *Alpha*, *Beta*, *Gamma*, *Mu* and *Nu* (Bernard et al. 2010). The nomenclature widely employed by the scientific community (de Villiers et al. 2004) names a species within each genus using a Greek letter with a number (e.g. *Alpha* papillomavirus-9) and the species are further subdivided into types which are defined by their genome having an L1 sequence which is at least 10% different from that of other types (e.g. HPV16). There is disagreement between this commonly accepted nomenclature and that officially employed by the International Committee on Taxonomy of Viruses (ICTV) which names a species based on one HPV type (e.g. HPV16) and all types within the species as strains instead (Bernard et al. 2010). Efforts are currently being made to reconcile the two systems (Bernard et al. 2010).

More than 150 HPV types have been described (Papillomavirus Episteme (PaVE); http:// pave.niaid.nih.gov/#home). Infections with high risk types of HPVs have the potential to cause cancerous lesions, whereas infections with low risk types are associated with causing benign lesions such as warts (Doorbar et al. 2012). The aetiological association between HPV and cancer was first elucidated by Dr. Harold zur Hausen and colleagues during the 1980s, when viral DNA was isolated from patient cervical tumour biopsies (Dürst et al. 1983) and from cervical carcinoma derived cell lines (e.g. HeLa) (Boshart et al. 1984). It is now known that virtually all cases of cervical cancer result from persistent infection by a high-risk HPV (Crow 2012). HPV16, belonging to the

species *Alpha* papillomavirus-9, is the most common high-risk type and is responsible for 54.4% of HPV related cervical cancers (Crow 2012). Hence, it is the focus of the following study. Additionally, high-risk HPVs have been implicated in 90% of anogenital cancers (Daling et al. 2004, Crow 2012, Forman et al. 2012) and also have an aetiological association with head and neck cancers (Crow 2012, Forman et al. 2012) as well as non-melanoma skin cancers (zur Hausen 1996).

Although vaccination against HPV types 16 and 18 is currently available (Gardasil® and Cervarix®) as well as cervical cancer screening via the Papanicolaou (Pap) test, HPV-related cancer still remains prevalent in populations with reduced access to these resources due to financial, cultural and geographical limitations (WHO 2010, Forman et al. 2012). This is a particularly relevant issue for members of the local First Nations communities here in Northwestern Ontario (Zehbe et al. 2011), highlighting the importance of further research into more targeted, less invasive treatments.

1.2 The HPV16 Genome and Viral Life Cycle

The HPV16 genome (**Figure 1**) is 7905 base pairs (bp) long (NCBI Accession #: NC_001526.2; Kennedy et al. 1991) and is maintained episomally within infected host cells (Doorbar 2005). It consists of a long control region (LCR) and encodes six early and two late expressed proteins (E1, E2, E4, E5, E6, E7, L1, and L2). The late proteins, L1 and L2, are expressed in the upper layers of the infected epithelium and compose the viral capsid (Doorbar 2005). The early proteins, E1, E2, E4, E5, E6, and E7, are mainly expressed in the lower and mid epithelial layers (Doorbar et al. 2012). The LCR region contains binding sites for cellular transcriptions factors as well as for the E1 and E2 proteins which initiate viral replication, control viral gene expression and help maintain

the virus episomally (Doorbar et al. 2012). The E4 and E5 proteins indirectly aid viral genome amplification, although it has been suggested that E4 may additionally play a role in facilitating viral particle release by weakening the keratin integrity of cells in the upper epithelial layer (Doorbar 2005, Doorbar et al. 2012). The E7 protein is most well-known for its ability to bind to and inactivate the retinoblastoma protein (pRb), leading to the release of the transcription factor E2F which causes entry into the S phase of the cell cycle and proliferation in the absence of normal growth factors (Klingelhutz and Roman 2012) (**Figure 2**). However, the key oncoprotein produced by the virus is E6.
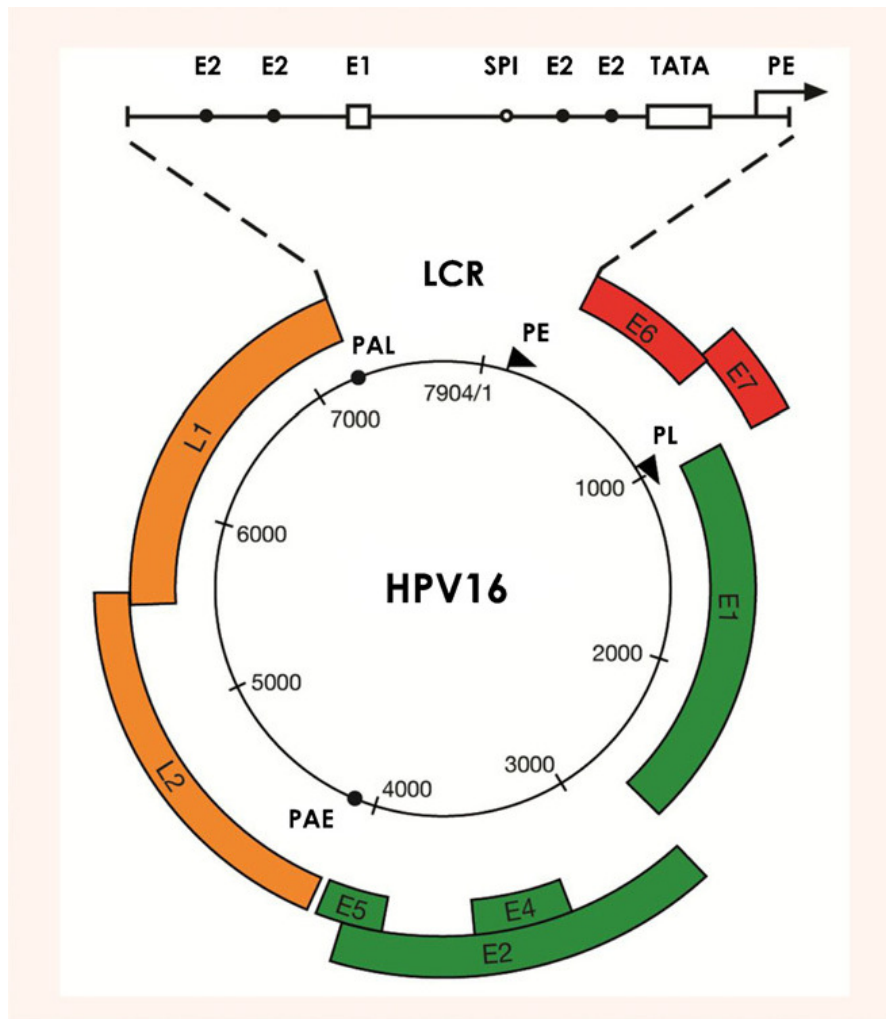
Figure 1. The HPV16 genome. A diagrammatic representation of the HPV16 genome demonstrating the location of the Long Control Region (LCR), the six early genes (E1, E2, E4, E5, E6 and E7), the two late genes (L1 and L2), the early (PE) and late (PL) promoters, and the early (PAE) and late (PAL) polyadenylation sites. Image taken from Doorbar et al. 2012

E6 is responsible for immortalizing and maintaining the malignant phenotype of infected cells as well as for aiding viral persistence through abrogation of the host's innate immune response (**Figure 2**) (as reviewed in Klingelhutz and Roman 2012). For example, the E6 protein, together with the ubiquitin ligase E6AP, binds to the tumour suppressor p53 protein leading to its ubiquitin-mediated degradation in the proteasome (Scheffner et al. 1993). In addition, E6 binds to the p300/CBP complex, preventing the acetylation of p53 and repressing its function in an E6AP independent manner (Patel et al. 1999, Zimmermann et al. 1999). This loss of p53 prevents the cell from entering apoptosis following DNA damage, allowing the accumulation of further potentially carcinogenic mutations. E6 also increases hTERT expression, the catalytic subunit of telomerase, which replenishes telomeres, protecting the chromosomes from damage during cell division and allowing the cells to become immortal (Veldman et al. 2003, Gewin et al. 2004, Katzenellenbogen et al. 2007, Sekaric et al. 2008). Cellular transformation to a malignant phenotype is facilitated by the ability of E6 to bind to and degrade PDZ domain containing proteins involved in cell-to-cell interactions, cell signaling and cell polarity, including MAGI-1 (Kranjec and Banks 2011), MAGI-2, MAGI-3 (Thomas et al. 2002), hScribble (Nakagawa and Huibregtse 2000), and hDlg (Kiyono et al. 1997, Gardiol et al. 1999). E6 aids in viral persistence through down regulation of the Type I interferons (IFN) α, β, (Ronco et al. 1998, Nees et al. 2001) and κ (Rincon-Orozco et al. 2009, DeCarlo et al. 2010, Reiser et al. 2011) as well as the Type II interferon, IFN γ (de Gruijl et al. 1999). A recent study by Niccoli et al. (2012) demonstrated that E6 could immortalize and malignantly transform keratinocytes in the absence of E7, further highlighting its role in the development of precancerous lesions.
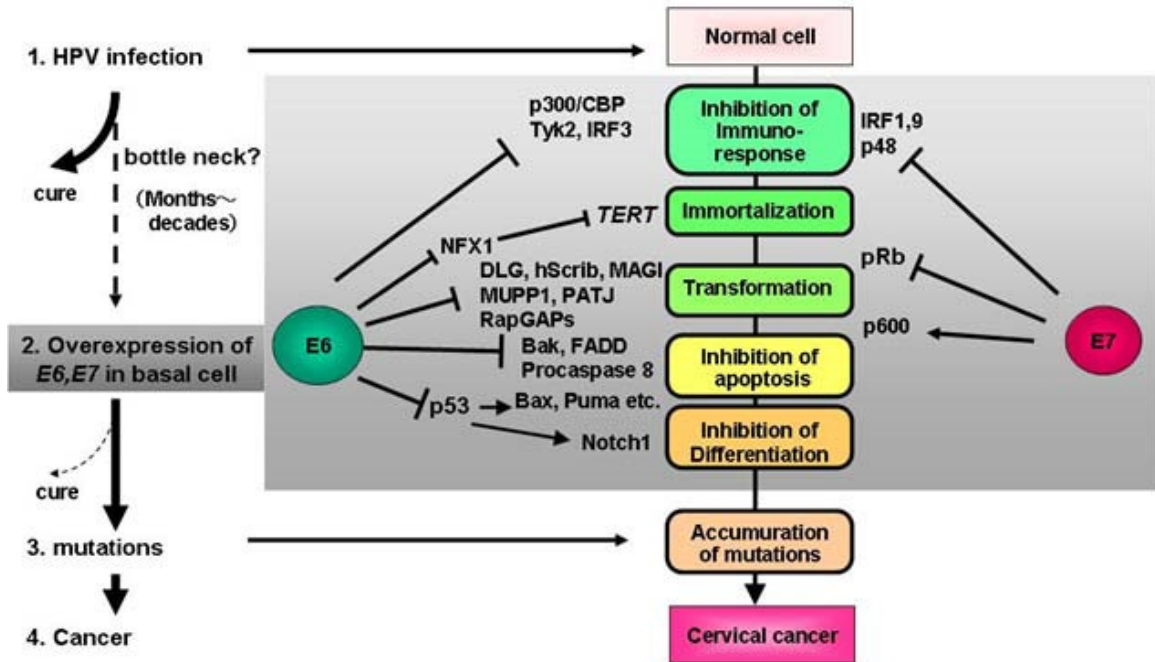
Figure 2. Cellular processes affected by HPV16 E6 and E7. A diagrammatic representation of the progression from HPV infection to cervical cancer, together with an overview of the accompanying cellular processes that are affected by the HPV16 E6 and E7 oncoproteins. Image taken from http://www.ncc.go.jp/en/nccri/divisions/10vir/10vir01.html.

HPV particles gain access to basal keratinocytes through microabrasions in the epithelium (**Figure 3**). Resulting from the actions of the above described viral proteins (particularly E6 and E7) infected keratinocytes abnormally continue proliferating in the suprabasal epithelial layers as viral replication occurs. Viral particles are released with the shedding of differentiated keratinocytes. The majority of HPV infections are cleared by the host's immune system (zur Hausen 2002). However, over the course of a persistent infection, the viral genome can become disrupted and integrated into the host genome. If disruption occurs in the E2 gene, E6 and E7 expression become subsequently upregulated and progression to high grade cervical intraepithelial neoplasia (CIN) or an invasive carcinoma can occur (Woodman 2007).
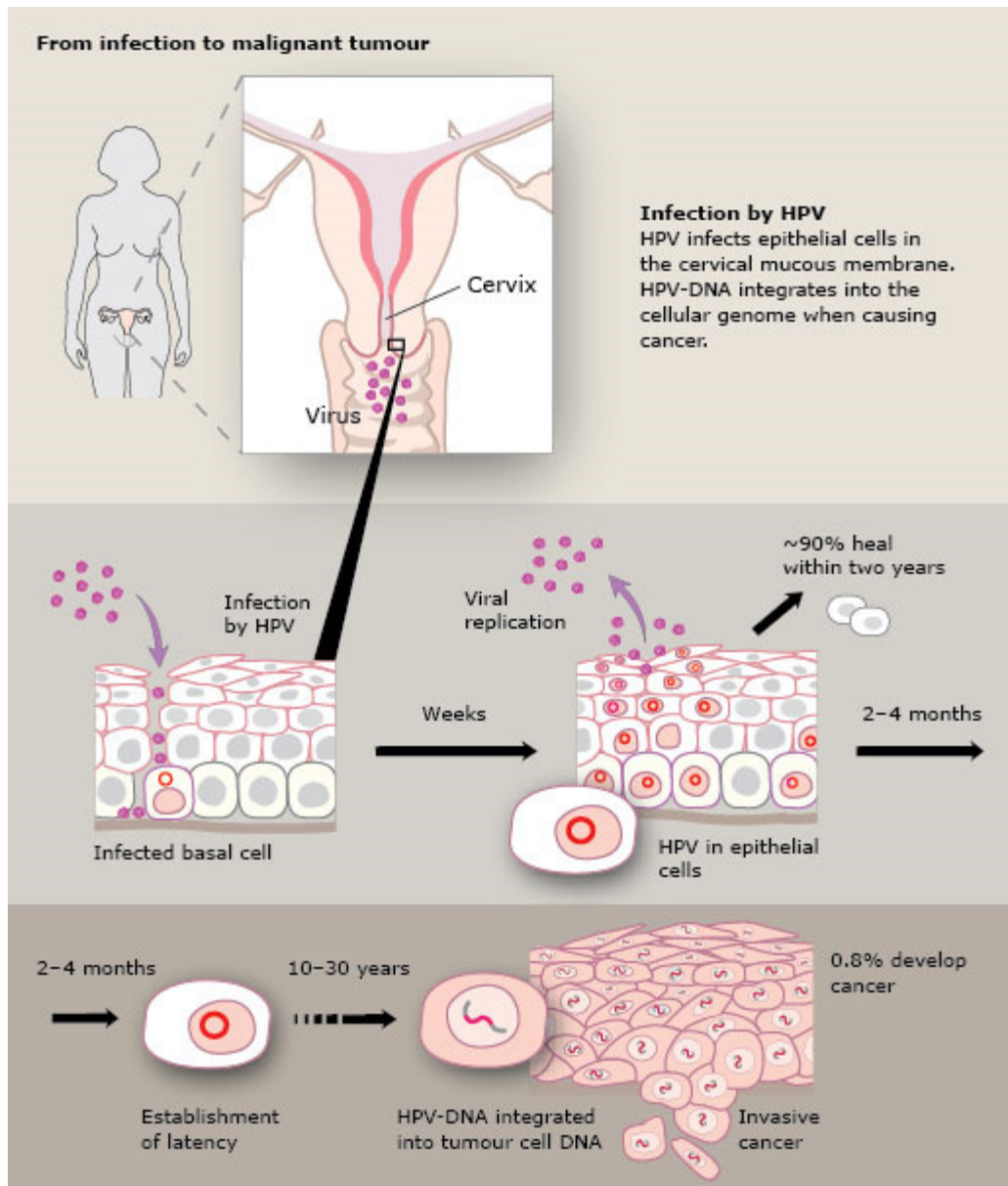
Figure 3. The HPV16 life cycle. An illustration demonstrating the progression from infection to cervical cancer. Most infections are eventually cleared by the host immune system. However, with persistent infection and integration of the virus into the host genome, the resulting upregulation of E6 and E7 expression can lead to cancer. Image taken from The 2008 Nobel Prize in Physiology or Medicine - Illustrated Presentation.

1.3 Current Treatments

Cervical intraepithelial neoplasias (CIN) are lesions of the cervix which develop following infection with the virus. These lesions are characterized by the presence of cells of a basal phenotype and abnormal proliferation persisting into the mid and upper layers of the epithelium, as well as disruption of the epithelium's normal stratified cytoplasmic differentiation pattern (Buckley et al. 1982, Woodman 2007). CIN are divided into low- to high-grade categories ranging from CIN I-CIN III (also known as carcinoma *in situ*) based on the neoplastic characteristics of the cells observed and the proportion (less than 1/3, 1/3-2/3, or greater than 2/3) of the epithelial layer involved (Buckley et al. 1982).

CINs are precursor lesions which can eventually progress to invasive carcinoma. However, the majority of these lower grade lesions will eventually be cleared by the host immune system (zur Hausen, 2002), leading care providers to favour an initial "watch and wait" approach (Singhania et al. 2012) where the patient is closely monitored with more frequent testing for several years following initial detection. However, this can cause considerable anxiety for the patient. If the infection is not cleared and the CIN progresses to a higher grade lesion, the affected area can be physically removed through a variety of methods including cryotherapy, laser ablation, or the loop electrosurgical excision procedure (LEEP), all of which are invasive and uncomfortable (Stern et al. 2012). The current standard of care for invasive cervical carcinoma is cisplatin chemotherapy combined with radiation therapy, which non-selectively destroys both healthy and cancerous cells (Stern et al. 2012), and may also require a hysterectomy including removal of the cervix. This results in unwanted side effects including nausea,

vomiting, as well as organ toxicity and has stark implications for women of a child bearing age.

1.4 HPV16 Targeted Treatments

1.4.1 Targeting HPV16 E6

Treatments capable of targeting the oncoproteins produced by HPV16 could potentially reverse the malignant phenotype of affected keratinocytes while sparing healthy cells. Since E6 is the main protein responsible for immortalization and maintenance of the malignant phenotype (Singhania et al. 2012), molecules capable of selectively blocking E6 expression are of particular interest to research.

E6 expression can be blocked at both the transcript and protein levels. Although E6 can be found within the cytoplasm of cells, the majority of this protein is located within the nucleus (Jackson et al. 2012) making it difficult to directly block using molecules, such as monoclonal antibodies, which are too large to passively diffuse into the nucleus (Pante et al. 2002, Togtema et al. 2012). Other molecules, capable of selectively targeting and degrading E6 mRNA and which only need to reach the perinuclear region of the cytoplasm, such as small interfering RNA (siRNA), are a more feasible, effective alternative.

1.4.2 RNA Interference (RNAi)

RNA interference (RNAi), first described by Fire et al. in 1998, is a mechanism by which plants and invertebrates are able to defend against viral infections (**Figure 4**). During various intermediate stages of replication for both RNA and DNA viruses, double-stranded RNAs (dsRNAs) can be formed (as reviewed in Voinnet 2005). These dsRNAs are cleaved into smaller fragments approximately 21-23 nucleotides in length,

known as small interfering RNAs (siRNAs), by the Dicer protein and the siRNAs then become incorporated into a group of proteins within the cell known as the RNA induced silencing complex (RISC) (Pecot et al. 2011). The siRNA is unwound, the sense (passenger) strand is removed, and the antisense (guide strand) binds through complete base pair complementarity to the corresponding viral mRNA (Pecot et al. 2011). Argonaute 2, an endonuclease contained within the RISC, then cleaves this transcript (Meister et al. 2004), preventing the translation of the viral protein. There has been considerable debate regarding whether RNAi still occurs as a natural response to viral infections in mammals (Voinnet 2005), however, mammalian cells are still able to respond to synthetically generated and transfected siRNAs, resulting in selective transcript degradation by the RISC (Elbashir et al. 2001) and making it a powerful potential therapeutic tool.
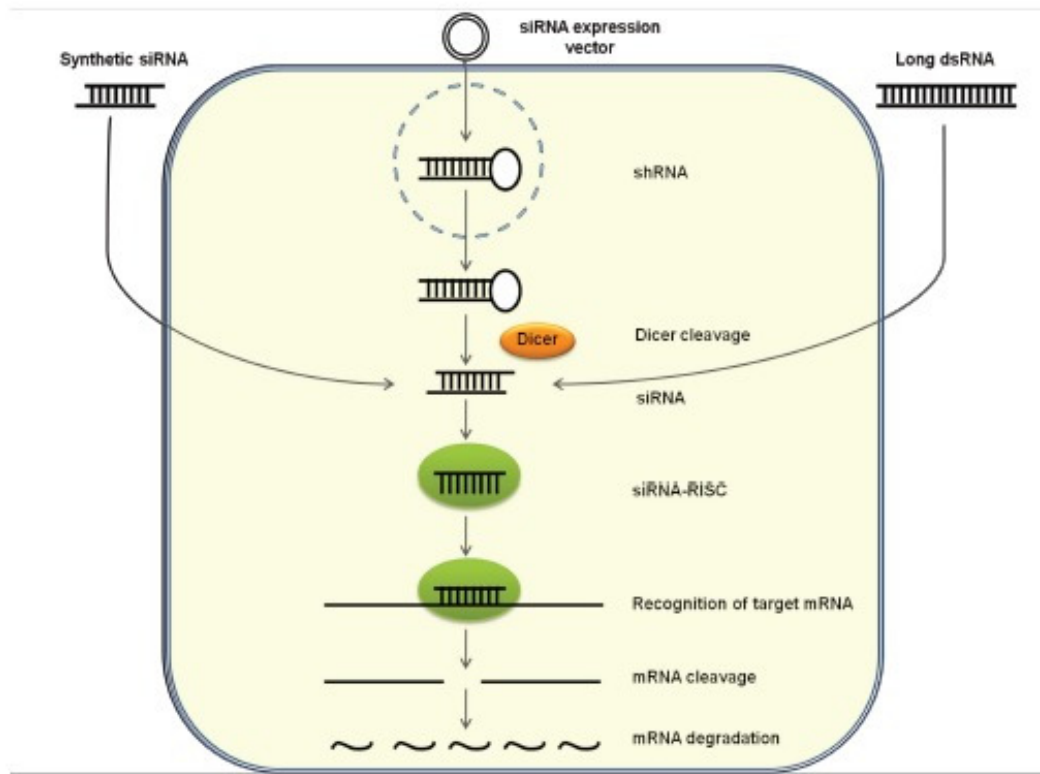
Figure 4. The mechanism of RNAi. Long dsRNA enters the cell as a product of a viral infection (top right) or expressed as shRNA from a vector (top centre) and is cleaved by Dicer into smaller fragments ~21-23 nucleotides long (siRNA). Alternatively, synthetic siRNAs can be transfected into the cell (top left), bypassing the need for Dicer cleavage. The siRNA is loaded into the RISC. The sense strand is discarded and the antisense strand guides the RISC to the target transcript, binding to it. The target transcript is then cleaved by the Argonaute 2 protein within the RISC. Image taken from Singhania et al. 2012.

1.4.3 HPV16 E6 siRNA

Following the discovery of RNAi, several studies emerged in the early 2000's investigating the use of synthetic siRNAs or vector expressed short-hairpin RNAs (shRNAs) to silence HPV16 E6 expression (as reviewed in Singhania et al. 2012). The curated database of experimentally validated siRNA/shRNA, VIRsiRNAdb (Thakur et al. 2012 and references therein), indicates that, to date, approximately 33 sequences targeting HPV16 E6 or E6/E7 expression have been developed and these sequences have had varying levels of success, depending on their target site on the mRNA, doses employed, and transfection strategies. For example, HPV16 E6 mRNA is bicistronic, sharing one transcript together with E7 (Smotkin et al. 1989). In addition, there are three splice variants of the transcript, E6-E7 mRNA, E6*I-E7 mRNA, and E6*II-E7 mRNA, where E6* indicates a portion of the E6 open reading frame (ORF) has been spliced out (**Figure 5**) (Smotkin et al. 1989). E6 can only be translated from the full-length transcript, whereas E7 can be translated from all three (Schneider-Gädicke and Schwarz 1986, Smotkin et al. 1989, Vaeteewoottacharn et al. 2005). To effectively suppress E6 while maintaining a minimal effect on E7, some groups have implemented siRNAs targeting the segment of E6 not present in the truncated transcripts (Butz et al. 2003, Courtête et al. 2007). Targeting this splice site (nt377-395), Butz et al. 2003 saw a restoration of p53 protein levels and the induction of apoptosis, 48 hrs following chemical transfection with approximately 120 nM siRNA. However, 48 hrs following chemical transfection with 10 nM of a similar siRNA sequence (nt386-404), Courtête et al. 2007 were only able to show a decrease in cellular proliferation accompanying p53 restoration. The study completed by Jiang and Milner in 2002 was one of the first to

show successful knockdown of HPV16 E6 mRNA, which lasted for 4 days following transfection, and restoration of cellular processes previously abrogated by the virus. Their siRNA sequence (nt224-242) targets the region just upstream and leading into the beginning of the splice site. A subsequent study then investigated the effects of targeting different locations along the E6 transcript using siRNAs designed with the same selection criteria and showed some siRNA sequences resulted in a higher E6 knockdown efficacy than others (Yamato et al. 2008). The authors suggested this may reflect easier accessibility of the RISC to certain target areas of the transcript than others. One of the most recent studies investigated HPV16 E6/E7 siRNA containing the motif "UXUCU" which was also capable of intentionally activating an immune response through the stimulation of TLR7 and subsequent Type I interferon production to aid in the therapeutic effect (Khairuddin et al. 2012).
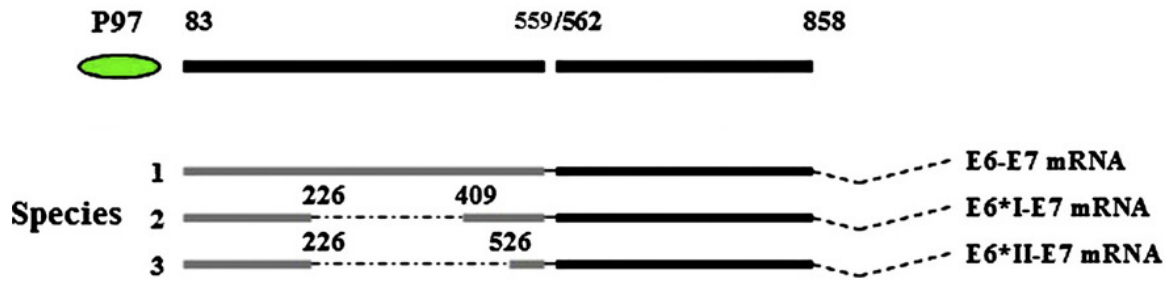
Figure 5. HPV16 E6/E7 mRNA. The HPV16 E6/E7 bicistronic transcript as well as its three splice variants. E6*I and E6*II indicate truncated E6. E6 is translated only from the full length transcript whereas E7 is translated from all three. Image modified from Zhou et al. 2012.

1.5 Modeling of mRNA Secondary and Tertiary Structures

Studies targeting insulin-like growth factor receptor (IGF1R) (Bohula et al. 2003), intercellular adhesion molecule-1 (ICAM-1)/CD54 (Kretschmer-Kazemi et al. 2003), and the genes of hepatitis C (HCV), influenza A, as well as human immunodeficiency virus (HIV) (Tan et al. 2012) have also demonstrated the ability of certain mRNA secondary structures to impair shRNA/siRNA knockdown efficiency. To aid in the prediction of target transcript areas which would be most accessible to the RISC, *in silico* models of mRNA secondary and tertiary structures can be constructed. Secondary structures such as helices, loops, bulges, junctions, and pseudoknots (Cristofari and Darlix 2002) mainly resulting from the canonical Watson-Crick base pairings of A-U, C-G, and G-U (Mathews 2006, Rivas 2013) are formed as RNA folds back on itself. These structures can be predicted using a variety of software. Some programs, including RNAfold (belonging to the well-known Vienna RNA package) (Hofacker 2003) and mfold (Zuker 2003), predict the structure with the lowest minimum free energy. Others rely on centroid estimators, such as the program CentroidFold (Sato et al. 2009). In the study by Kretschmer-Kazemi et al. 2003, mfold was used to predict the secondary structure of the ICAM-1 mRNA. siRNAs targeting regions of the transcript predicted to have strong base pairing had decreased knockdown efficacy compared to siRNAs targeting regions of the transcript predicted to be open loops, further demonstrating the accuracy and usefulness of these *in silico* approaches.

mRNA further folds into a tertiary structure influenced by non-canonical pairings between the nucleotides (e.g. hydrogen bonds involving the sugar) (Rivas 2013). Programs for modeling mRNA tertiary structures are less well-established than those for

determining protein tertiary structures, due to the difficulty in collecting experimental data to base them on. RNA is hard to crystallize (Kauffmann et al. 2009) and is challenging to purify in large amounts (Keel et al. 2007), complicating the use of x-ray crystallography. *In silico* programs including FARNA (belonging to the well-known Rosetta software package) (Das and Baker 2007) and iFoldRNA (Sharma et al. 2008) can be used to make initial predictions about RNA 3D structure. Force-fields as well as molecular dynamics parameters, including temperature, pH, and ions present in solution, can then be applied to simulate the stable minimum free energy of the RNA tertiary structure in the cellular environment, further optimizing the initially predicted structures. The outcome will ultimately be affected based on the inputs for these parameters which are chosen by the user (Shapiro et al. 2007).

1.6 Research Rationale

When considering treatment with an E6 siRNA, it is important to consider that the HPV16 E6 gene is polymorphic (Yamada et al. 1995, Zehbe et al. 1998). European Prototype (EP E6) and Asian-American (AA E6) are two common E6 variants. The AA E6 variant differs by six single nucleotide polymorphisms (SNPs) from EP E6 (Yamada et al. 1995) (**Figure 6**). Three of the SNPs (nt286 T>A, nt289 A>G, and nt532 A>G) are silent. The other three SNPs (nt145 G>T, nt335 C>T, and nt350 T>G) cause the amino acid substitutions glutamine-14-histidine, histidine-78-tyrosine and leucine-83-valine (Q14H, H78Y, and L83V) respectively. The variant SNPs can alter mRNA secondary structure (Shen et al. 1999), potentially affecting mRNA target accessibility and siRNA efficiency, and are mainly located in the E6 transcript splice site, a popular siRNA target.

17

In addition, epidemiological data indicate that the AA E6 variant is found more frequently in cervical cancer than EP E6 (Berumen et al 2001). Previous studies by our group have demonstrated that AA E6 is superior in immortalization and transformation abilities (Richard et al. 2010, Niccoli et al. 2012) and, in the context of the full viral genome, is superior at initiating early carcinogenesis in 3D raft cultures (Robert Jackson, Thunder Bay Regional Research Institute; personal communication). These differential functional abilities led our group to speculate that downstream cellular process may not be affected in the same way by EP and AA E6.

Here exists a knowledge gap. No previous study has quantified in detail the impact the variant E6 mRNA structures may have on siRNA knockdown efficacy and compared the response of subsequent downstream cellular pathways in each variant. Especially in the context of therapeutics, it is important to understand the difference in cellular responses when the same E6 siRNA is applied to each of the variants and may potentially highlight the need for different doses or sequences depending on whether the patient is infected with EP or AA E6.
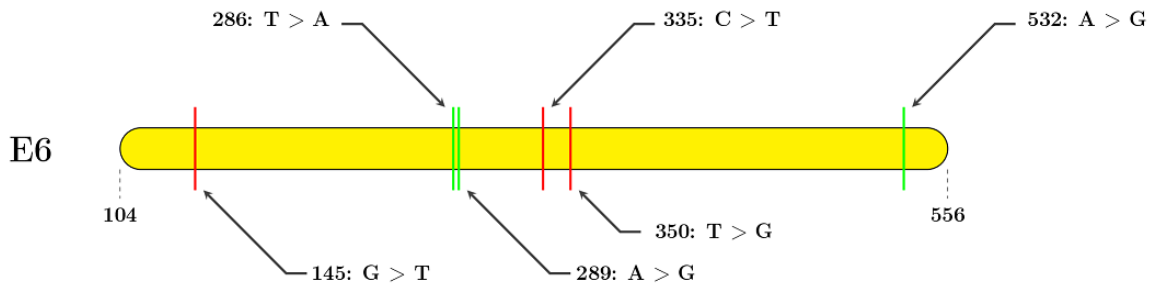
Figure 6. Single nucleotide polymorphisms of HPV16 AA E6. AA E6 differs from EP E6 by

six SNPs. Three SNPs (nt286 T>A, nt289 A>G and nt532 A>G), are silent (green). Three SNPs,

(nt145 G>T, nt335 C>T, and nt350 T>G), lead to the amino acid substitutions Q14H, H78Y and

L83V respectively (red).

1.7 Hypotheses

Therefore, based on the fact that AA E6 differs from EP E6 by these six SNPs, it was hypothesized that the E6 variant mRNA structures would be notably different from each other and that an E6 siRNA, despite targeting regions of the transcript with no base pair mismatches between the variants, would have significantly different silencing efficacies for cells containing EP versus AA E6. Due to the functional differences observed between EP and AA, it was also hypothesized that, once equal E6 knockdown of both variants was achieved, restoration of downstream cellular responses affected by E6 would be significantly different for each variant.

1.8 Research Aims

1. Create *in silico* models for the mRNA secondary and tertiary structures of both EP and AA E6.

2. Use primary human foreskin keratinocytes (PHFKs), which have been transduced with either the EP or AA variant of HPV16 E6 as an *in vitro* model.

   a. Chemically transfect the cells with an E6 siRNA which has no base pair mismatches between the variants. This siRNA will be chosen from existing, experimentally validated sequences to target an area predicted to be structurally different between EP and AA E6.

   b. Characterize E6 mRNA knockdown as well as the restoration of downstream cellular processes affected by E6 for each variant. Since hTERT expression is key for cellular immortalization and the abrogation of IFNs β, κ, and γ are important for viral evasion of the innate immune system, they are of particular interest to our group from a therapeutic

perspective. E6 protein levels, as well as those of the tumour suppressor protein p53, important for eliciting an apoptotic response, will also be quantified.

2 MATERIALS AND METHODS

2.1 Modeling of E6 mRNA Secondary and Tertiary Structures

The mRNA secondary structures for the EP and AA E6 variants was determined using the program CentroidFold (Sato et al. 2009). mRNA sequences were entered into the online webserver application (www.ncrna.org/centroidfold/). The default settings for model (CONTRAfold) and gamma (2^2) were employed.

The tertiary structure of the mRNAs was initially predicted using the program FARNA (Das and Baker 2007) (available at www.rosettacommons.org/software/). An energy term was added to favour the formation of the base-pairs predicted by CentroidFold for each E6 variant independently. Twenty predicted RNA structures were submitted to simulated annealing minimization until the energy converged under the Yamber3 force field as implemented in the program Yasara (www.yasara.org). The minimization protocol is described in detail elsewhere (Krieger et al. 2004). Charges were adjusted to reflect a pH of 7 and the final temperature for molecular dynamics was set to 37°C (310K) to simulate physiological conditions. Each RNA molecule was placed in a cell under periodic boundary conditions. Lennard-Jones forces and the direct space portion of the electrostatic forces were calculated using a cut-off of 7.86 Å. Electrostatic interactions were calculated using the Particle Mesh Ewald method as implemented in Yasara (www.yasara.org). An implicit solvation model (PBS) was used to report total potential and solvation energies. The most energetically favored resulting structure (i.e.

21

the structure with the most negative free energy) was then selected for each E6 mRNA variant. The 3D images were rendered using the open source program Jmol (Herráez 2006) (available at www.jmol.org/).

2.2 Cell Culture

2.2.1 Cell Lines and Routine Maintenance

Primary human foreskin keratinocytes (PHFKs; Cell Applications Inc, San Diego CA, USA, Cat. # 102-05n), retrovirally transduced with either the EP or AA variant of HPV16 E6 carrying a hemagglutinin (HA) tag on the C terminus, as previously described by Niccoli et al. 2012, were used for *in vitro* studies. All cells were greater than passage 30, ensuring they were well past any initial immortalization crises. Untransduced PHFKs were used as a control.

The cells were cultured in Serum-Free Keratinocyte Growth Medium (Cell Applications Inc., Cat. # 131-500) and were maintained at 37°C in a humidified incubator with 5% carbon dioxide gas. Culture medium was changed every second to third day. Cells were passaged when they reached 70-80% confluency, at which point they were incubated with trypsin (Fisher Scientific, Mississauga, ON, Canada, Cat. # SH3023602) until they detached. The trypsin was neutralized with Neutralizing Solution (Cell Applications Inc., Cat. # 080-100). The Neutralizing Solution was removed by centrifugation at 25 x g (GS-6KR Centrifuge; Beckman, Mississauga, ON, Canada) for 5 minutes, the supernatant was aspirated from the pellet, and the pellet was then resuspended in fresh medium.

Cells were routinely screened for *Mycoplasma* contamination at every second passage. The cells were grown on sterile glass coverslips (Fisher Scientific, Cat. # 12-

541A) for 2-3 days and then fixed using 3 parts methanol (Fisher Scientific, Cat. # A4544) and 1 part glacial acetic acid (Sigma-Aldrich-Aldrich, Oakville, ON, Canada, Cat. # 695092-2.5L) for 15 minutes. The coverslips were mounted using Vectashield medium with DAPI (Vector Laboratories, Burlington, ON, Canada, Cat. # H-1200), to stain the DNA fluorescent blue. The slides were examined using an inverted Zeiss Axiovert 200 microscope (Carl Zeiss Canada Ltd., North York, ON, Canada) at 400x magnification for the presence of *Mycoplasma* DNA in the cytoplasm of the cells. No issues with *Mycoplasma* contamination were noted throughout the study.

2.2.2 Cryogenic Cell Storage

To preserve stocks of cells, freezebacks were made. Neutralizing Solution was removed from trypsinized cells by centrifugation at 25 x g (GS-6KR Centrifuge; Beckman) for 5 minutes followed by aspiration of the supernatant. The cell pellet was then resuspended in a solution consisting of 90% culture medium and 10% dimethyl sulfoxide cryopreservative (DMSO; Sigma-Aldrich-Aldrich, Cat. # 34869). Aliquots of 1 mL were placed in Nalgene 1.5 mL cryogenic vials (Fisher, Cat. # 03-337-7Y). The cryogenic vials were frozen in a Nalgene controlled rate freezing container (Fisher, Cat. # 5100-0001) at -80 °C and were then transferred into liquid nitrogen for long term storage.

2.2.3 Thawing Cells

To bring up cells from cryogenic storage, the cryogenic vial was removed from the liquid nitrogen and immediately thawed in a 37°C bath. The contents of the cryogenic vial were added directly to 14 mL of culture medium, to dilute the concentration of DMSO to non-toxic levels for the cells. The cells were added to the growth flask(s) and

placed into the incubator. The culture medium was changed the following morning after the cells had adhered, to remove any traces of DMSO.

2.3 DNA Sequencing

2.3.1 Cell Preparation

Cells were cultured in a T75 (75 cm^2) flask (Fisher, Cat. # 1368065) and were trypsinized from the flask as described above. Following removal of the Neutralizing Solution, the cell pellet was resuspended in 2 mL DPBS (Fisher, Cat. # SH3002802) and cells were counted using a TC10™ Automated Cell Counter (BioRad, Mississauga, ON, Canada). The suspension was centrifuged for 5 min at 25 x g (GS-6KR Centrifuge; Beckman) and the DPBS was removed from the cell pellet. The dry cell pellet was stored at -80 °C until DNA extraction.

2.3.2 DNA Extraction and PCR

DNA was extracted from the cells using the DNeasy® Blood and Tissue Kit (Qiagen, Toronto, ON, Canada, Cat. # 69504). The final DNA elution was done using 2 x 100 µL of Buffer AE. DNA was quantified using the Synergy 4 spectrophotometer (BioTek, Winooski, VT, USA) and Take3 micro-volume plate, with the elution buffer as a blank sample. Absorbance measurements at wavelengths of 260 and 280 nm were taken, which provided the purity of the DNA sample ($A_{260/280}$) and the concentration in ng/µL.

To amplify the HPV16 E6 DNA, PCR was performed. Twenty-five µL reactions were mixed, consisting of 100 ng template DNA, 1x PCR Buffer, 200 µM dNTPs, 2 U Taq Polymerase, 1 mM MgCl$_2$, 0.5 µM E6 forward primer (5'-CAATGTTTCAGGACCCACA-3'), 0.5 µM E6 reverse primer

24

(5'GTTTCTCTACGTGTTCTTGA-3'), and nuclease-free dH_2O to bring the mixture up to the final volume. Control reactions, which contained nuclease-free dH_2O instead of template DNA were also mixed. The reactions were run in a 2720 Thermal Cycler (Applied Biosystems, Burlington, ON, Canada) using the following parameters: 40 cycles of 1 min 94 °C denaturation, 1 min 56 °C annealing and 2 min of 72 °C extension. The final extension was for 7 min at 72 °C followed by an infinite hold at 4 °C.

2.3.3 Agarose Gel Electrophoresis and Post-PCR Purification

To visualize the 448 bp E6 amplicon, agarose gel electrophoresis was utilized. A 1.5% agarose gel (PCR agarose; BioRad, Cat. # 161-3104) was mixed with 1X Tris/Borate/EDTA (TBE) buffer (100 mL 10X TBE and 900 mL dH_2O) and 0.5 µg/mL of ethidium bromide (Invitrogen, Burlington, ON, Canada, Cat # 15585-011). The 10X TBE buffer consisted of 108 g Tris Base (Sigma-Aldrich, Cat. # T1503-1KG), 55 g boric acid (Sigma-Aldrich, Cat. # B7901-500G), 40 mL 0.5 M ethylenediaminetetraacetic acid (EDTA) (Fisher, Cat. # BP120-1) dissolved in 1 L dH_2O and autoclaved for 20 minutes. The gel was cast in a mini-gel apparatus and allowed to polymerize for 45 min. Two µL of 6x loading dye (Fermentas, Mississauga, ON, Canada, Cat. #R0611) was mixed with 10 µL of each sample before loading onto the gel. Ten µL of a 100 bp DNA ladder (New England BioLabs, Whitby, ON, Canada, Cat. # N0467), as well as positive and negative control samples were also loaded. The gel was run at 100 V for 1 hour and then imaged with 365 nm transillumination using a UV imager (Biospectrum 410 Imaging System; UVP, Upland, CA, USA). Images were captured using a 0.1s exposure.

The post-PCR products were then purified to remove primer dimers and any degraded DNA. Given the presence of a non-specific band at ~800 bp in the AA E6

sample which could not be diminished despite attempts to optimize the PCR parameters, the AA E6 band was excised from the gel using a scalpel and the DNA purified using the QIAquick Gel Extraction Kit (Qiagen, Cat. # 28704). For EP E6, the remaining PCR amplified DNA sample not run on the above gel was purified using the QIAquick PCR Purification Kit (Qiagen, Cat. # 28104). Both samples were eluted in 50 µL nuclease-free dH$_2$O (pH 7.5). Due to some sample loss during the purification process, the DNA was re-quantified as described above. Samples of 20 ng each were run on a 1.5% agarose gel as described above to ensure removal of the non-specific amplicon and primer dimers had occurred. The purified DNA samples were stored at -20 °C until sequencing.

2.3.4 E6 Variant Sequencing

The DNA samples were diluted to a concentration of 2 ng/µL and the above described E6 forward and reverse primers to a concentration of 10 µM. A 10 µL volume of each sample along with 10 µL of both the forward and reverse primers were then sent to the Paleo-DNA Laboratory at Lakehead University, Thunder Bay, ON, Canada for Sanger sequencing using dye terminator chemistry (3130xl Genetic Analyzer; Applied Biosystems). Both forward and reverse reads were obtained for each sample. The reads were combined together to create a consensus sequence using BioEdit software (Hall 1999). The DNA sequence trace chromatograms were manually scanned for base miscalls and to clarify undetermined bases (indicated by an "N" in the sequence). The consensus sequences for each variant were then compared to the original sequences transduced into the cells (Niccoli et al. 2012) for confirmation.

2.4 siRNA

siRNA duplexes were custom synthesized by Sigma-Aldrich-Aldrich and were reconstituted in nuclease-free dH$_2$O to a stock concentration of 2 µM. An E6 siRNA containing no base pair mismatches with either variant but targeting a region of the transcript predicted *in silico* to be structurally different between EP and AA E6 was chosen from existing, experimentally validated E6 siRNA sequences. This E6 siRNA, described by Courtête et al. 2007, would target the splice site of the E6 transcript, leaving E7 expression intact in cells containing the entire viral genome. A scrambled version of the E6 siRNA, having no target transcript within the cell, was used as a negative treatment control. See **Table 1** for the sense and antisense sequences.

Table 1. siRNA sequences used in this study.

Sequence	Sense Strand	Anti-Sense Strand
E6 siRNA (nt386-404)	5' CCGUUGUGUGAUUUGUUAA[dT][dT] 3'	5' UUAACAAAUCACACAACGG[dT][dT] 3'
Scrambled siRNA	5' UAUGUGCUAUGUAUUAUUG[dT][dT] 3'	5' CAAUAAUACAUAGCACAUA[dT][dT] 3'

2.5 Relative mRNA Expression

2.5.1 Chemical Transfection with siRNA

Twenty-four hours before transfection with siRNA, EP E6, AA E6, as well as untransduced PHFKs were seeded into 6-well plates (Fisher Scientific, Cat. # 087721B) at a concentration of 200 000 cells/well for the EP E6 and AA E6 cells and 150 000 cells/well for the untransduced PHFKs. The following day when the cells had reached a starting confluency of ~50%, the culture medium was aspirated and replaced with 3 mL of fresh culture medium. Transfection complexes of 600 µL were mixed for each well. To give a final concentration of 10 nM siRNA in the well, each complex consisted of 18 µL HiPerFect chemical transfection reagent (a mixture of cationic and neutral lipids) (Qiagen, Cat. # 301705), 18 µL 2 µM E6 or scrambled siRNA stock, and 564 µL culture medium. To give a final concentration of 25 nM siRNA in the well, each complex consisted of 18 µL HiPerFect chemical transfection reagent, 45 µL 2 µM E6 or scrambled siRNA stock, and 537 µL culture medium. The complexes were mixed by vortexing, incubated at room temperature for 10 minutes and then added drop-wise to the wells. The plates were gently swirled to ensure even distribution of the complexes and were returned to the incubator for forty-eight hours. Untransfected cells (i.e. treated with medium only) were used to determine baseline E6 mRNA levels. All transfections were repeated in biological triplicate (i.e. 3 wells).

2.5.2 RNA Extraction

Forty-eight hours following transfection, the cells were harvested from the 6-well plates using trypsin as described above and any remaining cells were rinsed from the wells using 1 mL DPBS (Fisher, Cat. # SH3002802). Following removal of the

Neutralizing Solution, each cell pellet was resuspended in 2 mL DPBS (Fisher, Cat. # SH3002802) and the number of cells remaining in each well were counted using a TC10™ Automated Cell Counter (BioRad). Each sample was centrifuged for 5 min at 25 x g (GS-6KR Centrifuge; Beckman) and the DPBS was removed from each cell pellet. The dry cell pellet was frozen at -80 °C until RNA extraction.

RNA extraction was performed using the Arctus PicoPure RNA Isolation Kit (Applied Biosystems, Cat. # KIT0204). The optional DNase treatment (RNase-free DNase Set; Qiagen, Cat. # 79254) step was included and all samples were eluted in 30 µL of elution buffer. All samples were stored at -80 °C until conversion to cDNA.

The quantity of the RNA in ng/µL as well as its integrity, as assessed by the 28S:18S ratio, was determined using the Experion Automated Electrophoresis System (BioRad) and the StdSens Analysis chip kit (BioRad, Cat. # 700-7111). All samples with an RNA quality indicator (RQI) value of less than 7 were flagged as being potentially degraded.

2.5.3 Conversion of RNA to cDNA

Each RNA sample was reverse transcribed into complementary DNA (cDNA) using the High Capacity cDNA Archive Kit (Applied Biosystems, Cat. # 4322171) in a 60 µL reaction. The volume of eluted RNA was brought up to 30 µL using nuclease-free dH$_2$O and added to 30 µL of 2X master mix. The 2X master mix contained 2X RT Buffer, 2X random primers, 2X dNTPs, multiscribe enzyme, and nuclease-free dH$_2$O to raise the final volume to the correct amount. The reactions were run in a 2720 Thermal Cycler (Applied Biosystems) using the following parameters: 10 min 25 °C, 120 min 37

°C, 5 min 85 °C and an infinite hold at 4 °C. All cDNA samples were stored at -20 °C

until real-time reverse transcription polymerase chain reaction (RT-qPCR) analysis.

2.5.4 Real-Time Reverse Transcription Polymerase Chain Reaction Analysis of Relative mRNA Expression

RT-qPCR analysis (7500 Real-Time PCR System; Applied Biosystems) was used

to determine the change in the relative expression of HPV16 E6, hTERT, IFN β, IFN κ,

and IFN γ mRNA in response to treatment of the cells with E6 or scrambled siRNA.

Hypoxanthine phosphoribosyltransferase 1 (HPRT1) was used as the reference gene, as

previous studies by our group have shown its expression to remain unchanged in

response to HPV infection (DeCarlo et al. 2008). Reactions of 90 µL were mixed

containing 45 µL of Taqman® Universal PCR Master Mix (Applied Biosystems, Cat. #

4364338), 4.5 µL of 20X Taqman® Gene Expression Assay (Applied Biosystems, **Table

2**), 150 ng cDNA, and nuclease-free dH$_2$O to raise the final volume to the correct amount.

Twenty-five µL of the reaction mixture was loaded into each of 3 wells on a MicroAmp®

Optical 96-Well Reaction Plate (Applied Biosystems, Cat. # 4306737). Positive tumour

controls and negative nuclease-free dH$_2$O controls containing the HPRT1 Gene

Expression Assay were run as technical controls on each plate as well. Cycle threshold

(Ct) data was analyzed relative to HPRT1 and calibrated to cells treated with scrambled

siRNA ($2^{-\Delta\Delta Ct}$; Livak and Schmittgen 2001).

Table 2. RT-qPCR TaqMan® Gene Expression Assays used in this study.

TaqMan® Gene Expression Assay	Assay ID Number
HPRT1	Hs99999909_m1
HPV16 Full Length E6*	AI0IW1V
HPV16 Full Length AA E6*	AIWR2XO
IFN β	Hs00277188_s1
IFN κ	Hs00737883_m1
IFN γ	Hs00174143_m1

*Custom designed assay.

2.6 Human Influenza Hemagglutinin (HA) Western Blot

2.6.1 Chemical Transfection with siRNA

EP E6, AA E6, as well as untransduced PHFKs were grown in T25 (25 cm^2) flasks (Fisher Scientific, Cat. # 101269) until they reached ~65% confluency. The culture medium was aspirated and replaced with 5 mL of fresh culture medium. Transfection complexes of 1 mL were mixed for each flask. To give a final concentration of 10 nM siRNA in the flask, each complex consisted of 30 µL HiPerFect chemical transfection reagent, 30 µL 2 µM E6 or scrambled siRNA stock, and 940 µL culture medium. To give a final concentration of 25 nM siRNA in the flask, each complex consisted of 30 µL HiPerFect chemical transfection reagent, 75 µL 2 µM E6 or scrambled siRNA stock, and 895 µL culture medium. The complexes were mixed by vortexing, incubated at room temperature for 10 minutes and then added drop-wise to the flasks. The flasks were gently swirled to ensure even distribution of the complexes and were returned to the incubator for forty-eight hours.

2.6.2 Protein Extraction

Forty-eight hours following transfection, the cells were harvested from the flasks using trypsin as described above. Following removal of the Neutralizing Solution, each cell pellet was resuspended in 4 mL DPBS (Fisher, Cat. # SH3002802). Each sample was centrifuged for 5 min at 25 x g (GS-6KR Centrifuge; Beckman) and the DPBS was removed from each cell pellet. Lysis buffer composed of 1 mL modified RIPA buffer (50mM Tris-HCl (pH 7.5), 5 mM EDTA, 150 mM sodium chloride (Fisher, Cat. # S2713), 1% Triton X-100 (Fisher, Cat. # BP151-100), 10 mM sodium fluoride (Fisher, Cat. # S299-100), and 20 mM β-mercaptoethanol (Sigma-Aldrich, Cat. # M6250-

100ML)), 10 μL phenylmethylsulfonyl fluoride (PMSF; Sigma-Aldrich, Cat. # P7626), 10 μL protease inhibitor cocktail (Sigma-Aldrich, Cat. # P8340), and 12 μL of activated sodium orthovanadate (Sigma-Aldrich, Cat. # S6508-50G) was mixed and chilled at 4 °C. Each fresh pellet was resuspended in 110 μL of the chilled lysis buffer and left on ice and in the 4 °C fridge for 20 minutes. The solutions were centrifuged for 1 minute at 14 000 rpm in a microcentrifuge pre-chilled to 4 °C (Centrifuge 5415C; Eppendorf, Mississauga, ON, Canada) to remove cell debris and obtain the protein containing supernatant.

A Bradford assay was done to determine protein concentration. A 5 μL volume of each sample and 100 μL BioRad Protein Assay Dye Reagent Concentrate (BioRad, Cat. # 500-0006) were mixed with 400 μL dH$_2$0. Various concentrations of bovine serum albumin (BSA) were used as the standards. The reactions were incubated on ice for 5 minutes and then 300 μL of each mixture was transferred to a 96-well plate (Fisher, Cat. # 087722c) where the protein concentration was analyzed using a plate reader (PowerWave XS; BioTek).

2.6.3 Gel Electrophoresis

SDS-PAGE gels were cast. A 15% separating gel was mixed first, containing 3.75 mL 40% acrylamide (BioRad, Cat. # 161-0146), 2.5 mL 1.5 M Tris-HCl (pH 8.8), 100 μL 10% sodium dodecyl sulphate (SDS) (Sigma-Aldrich, Cat. # L3771-100G), 3.6 mL dH$_2$O, 10 μL tetramethylethylenediamine (TEMED) (Sigma-Aldrich, Cat. # T7024), and 60 μL 10% ammonium persulfate (APS) (Sigma-Aldrich, Cat. # A9164). The separating gel was settled with isopropyl alcohol and allowed to polymerize for 15 minutes. The isopropyl alcohol was removed and then the 4% stacking gel, consisting of 0.5 mL 40% acrylamide, 1.26 mL 0.5 M Tris-HCl (pH 6.8), 3.18 mL dH$_2$O, 10 μL TEMED, and 40

34

μL 10% APS was added on top. The comb was inserted and the stacking gel was allowed to polymerize for 30 minutes.

One hundred μg of protein was mixed with 6X SDS for each sample. All samples were brought up to the highest sample volume using 1X SDS. The SDS containing samples were heated at 95 °C for 5 minutes to denature the protein. The BioRad Prestained SDS-PAGE Low Range Standards (BioRad, Cat. # 161-0305) (heated for 2 min) as well as the BioRad Precision Plus Protein WesternC Standards (BioRad, Cat. # 161-0376) (not heated) were used for protein ladders. All samples and standards were centrifuged for 1 minute at 14 000 rpm (Centrifuge 5415C; Eppendorf) and loaded onto the gel. The gel was run in 1X running buffer (100 mL 10X running buffer and 900 mL dH$_2$0) at 100 V for 20 minutes until the samples reached the separating gel. The 10X running buffer consisted of 144 g glycine (Fisher, Cat. # BP381-5), 30.3 g Tris Base, and 50 mL 10% SDS made up to 1L in dH$_2$0. The current was then turned up to 120 V and the gel was run from another 1 hour and 20 minutes, until the dye front ran just off the bottom of the gel.

2.6.4 Transfer

Following the completion of the run, the proteins were transferred to PVDF membrane (Fisher, Cat. # PI88518) which had been activated by soaking in methanol (Fisher, Cat. # A4544) for 15 minutes. The transfer was done at 100 V for 1 hour in chilled 1X transfer buffer (100 mL 10X transfer buffer, 200 mL methanol and 700 mL dH$_2$0) with an ice pack and a stir bar in the container to keep the temperature cool. The 10X transfer buffer consisted of 144 g glycine and 30.3 g Tris Base made up to 1 L in dH$_2$0. Following the transfer, the membrane was soaked in 1X TBS with 0.05%

TWEEN® 20 (Fisher, Cat. # 337-100) (TBST) for 10 minutes. The 10X TBS consisted of 30.3 g Tris Base and 87.6 g sodium chloride made up to 1 L in dH_20 (pH 7.5). The membrane was then cut between the 25 and 37 kDa markers on the Precison Plus ladder and between the 29 and 36 kDa markers on the Low Range ladder allowing for actin (top half of membrane) and HA (bottom half of membrane) to be detected simultaneously.

2.6.5 Actin and HA Detection

Both membrane halves were blocked with 5% milk powder in TBST for 1 hour at room temperature on a rocker. The top half of the membrane was then incubated with a goat polyclonal actin primary antibody (Santa Cruz, Dallas, TX, USA, Cat. # SC-1616) diluted 1:1000 in 5% milk powder. The bottom half of the membrane was incubated with a mouse monoclonal HA primary antibody (Abcam, Toronto, ON, Canada, Cat. # ab18181). The incubation was done by placing the membrane halves and antibody solutions in 50 mL tubes (Fisher, Cat. # 1443222) on a tube roller overnight at 4 °C.

The following morning, the membrane halves were rinsed once in TBST and then were washed 4 x 5 minutes in TBST on a rocker. The top half of the membrane was incubated with the StrepTactin-horseradish peroxidase (HRP) conjugate (BioRad, Cat. # 161-0381) for the Precision Plus ladder and a donkey anti-goat+HRP secondary antibody (Jackson ImmunoResearch, West Grove, PA, USA, Cat. # 705-035-147) diluted 1:2000 in 5% milk powder. The bottom half of the membrane was incubated with the StrepTactin-HRP conjugate for the Precision Plus ladder and a goat anti-mouse+HRP secondary antibody (Jackson ImmunoResearch, Cat. # 115-035-062) diluted 1:2000 in 5% milk powder. The incubation was for 1 hour at room temperature on a rocker. The

membranes were then rinsed again in TBST and washed 4 x 5 minutes in TBST on a rocker.

Chemiluminescence was done using the Western Lightening®-ECL kit (PerkinElmer, Waltham, MA, USA, Cat. #NEL100001EA). One mL of each of the two solutions was mixed together and applied to each membrane half for 1 minute. The membrane halves were then directly imaged using the Biospectrum 410 Imaging System (UVP) with a 10 minute exposure for HA and a 2 minute exposure for actin.

2.7 p53 Protein Detection Using Quantitative Immunofluorescence

2.7.1 Chemical Transfection with siRNA

Twenty-four hours before transfection with siRNA, EP E6, AA E6, as well as untransduced PHFKs were seeded into 24-well plates (Fisher Scientific, Cat. # 087721) at a concentration of 50 000 cells/well. The following day when the cells had reached a starting confluency of ~50%, the culture medium was aspirated and replaced with 500 µL of fresh culture medium. Transfection complexes of 100 µL were mixed for each well. To give a final concentration of 10 nM siRNA in the well, each complex consisted of 3 µL HiPerFect chemical transfection reagent, 3 µL 2 µM E6 or scrambled siRNA stock, and 194 µL culture medium. To give a final concentration of 25 nM siRNA in the well, each complex consisted of 3 µL HiPerFect chemical transfection reagent, 7.5 µL 2 µM E6 or scrambled siRNA stock, and 89.5 µL culture medium. The siRNA for this experiment possessed a carboxyfluorescein (6-FAM) label on the 5' end of the sense strand, allowing for visual confirmation of transfection. Wells treated with the transfection reagent only or medium only were also included as controls. The complexes were mixed by vortexing, incubated at room temperature for 10 minutes and then added

37

drop-wise to the wells. The plates were gently swirled to ensure even distribution of the complexes and were returned to the incubator for forty-eight hours. All transfections were repeated in biological triplicate (i.e. 3 wells).

2.7.2 Immunofluorescence Staining

Forty-eight hours following transfection, the culture medium was aspirated from the wells. The cells were rinsed once with DPBS and then fixed with 500 µL/well of 4% paraformaldehyde (PFA) (Fisher, Cat. # O4042500) in PBS for 10 minutes at room temperature. The cells were washed 3 x 5 minutes with PBS and the plates were stored at 4 °C with the last wash remaining in the wells until staining.

The cells were permeabilized with 0.1% Triton X-100 in PBS for 5 minutes at room temperature and then rinsed once in PBS. Blocking was done with 1% BSA in PBS for 10 minutes at room temperature. A rabbit monoclonal p53 primary antibody (DAKO, Burlington, ON, Canada, Cat. # M3629) diluted 1:100 in 1% BSA-PBS was applied to the cells. Staining controls received only 1% BSA-PBS but no primary antibody. The primary antibody was incubated overnight at 4 °C.

The following day, the primary antibody was removed from the wells. The cells were rinsed once with chilled PBS and then washed 3 x 5 minutes with chilled PBS. The cells were equilibrated with 1% BSA-PBS for 10 minutes at room temperature. A donkey anti-rabbit secondary antibody conjugated with Alexa Fluor® 594 (Invitrogen, Cat. # A-21207) diluted at 1:800 was then applied and incubated for 30 minutes at room temperature in the dark. Again, the cells were rinsed once in PBS and then washed 3 x 5 minutes with PBS. Following a final rinse in dH_2O, ~150 µL of dH_2O and 1 drop of Vectashield with DAPI were added to each well and let sit for 5 minutes to stain the

DNA fluorescent blue. The solution was aspirated from the wells and 100 µL of dH₂O was added to each well before imaging.

2.7.3 Microscopy and Quantitation

Fluorescent microscopy at 400x magnification was performed using a Zeiss Axiovert 200 Microscope (Carl Zeiss Canada Ltd.) equipped with a LD A-Plan 40x/0.50 Ph2 objective (Carl Zeiss Canada Ltd.) and a CCD camera with 12 bit capability (Q Imaging, Surrey, BC, Canada). All images were captured by an undergraduate student in the lab blinded to the experiment and any expected outcomes, to prevent bias. Using the correct microscope filters, 5 pairs of images (1 DAPI and 1 p53) were taken within each well in a pattern to cover as many areas as possible. DAPI has an excitation at ~360 nm and emission at ~460 nm (blue). Alexa Fluor® 594 has an excitation ~590 nm and emission at ~617 nm (red). For DAPI and p53 images, exposures of 100 ms and 800 ms were used respectively. The gain was set to 2.26% and the offset to 50.01% for all images.

The percent p53 positive cells in each well were quantified by determining the number of Alexa Fluor® 594 stained cells as well as the total number of cells, indicated by DAPI staining. To do this, the images were digitally processed using CellProfiler open source software (Carpenter et al. 2006), a program which can be used for both the objective quantification and subcellular localization of protein expression in the same experimentally treated cells (Carpenter et al. 2007, Hamilton 2009, Togtema et al. 2012, Jackson et al. 2013). First, the DAPI images were used to identify the nuclei (objects) in the field of view. An image mask was drawn around each nucleus and overlaid on the corresponding p53 image (**Figure 7A**). The intensity of p53 staining (red) for each

nucleus was then quantified within that mask. The average and standard deviation of any

red background fluorescence was also calculated in the areas not covered by nuclei for

each photo (**Figure 7B**). In each field of view, a cell was considered p53 positive if the

mean red signal intensity of its nucleus was larger than the mean red background signal

intensity plus three standard deviations. The pipeline of program steps was as follows:

"Load Images", "Resize", "Colour To Gray" (for DAPI), "Colour To Gray" (for p53),

"Identify Primary Objects", "Convert Object To Image", "Image Math", "Apply

Threshold", "Identify Primary Objects" (identifies background), "Measure Object

Intensity" (of nuclei), "Measure Object Intensity" (of background), "Overlay Outlines",

"Display Data on Image" (shows number of nuclei), "Display Data on Image" (shows

intensity of nuclei), and "Export Data to Spreadsheet". The exported intensity data was

then manually analyzed in Excel based on the above threshold criteria to determine the

number of p53 positive cells.
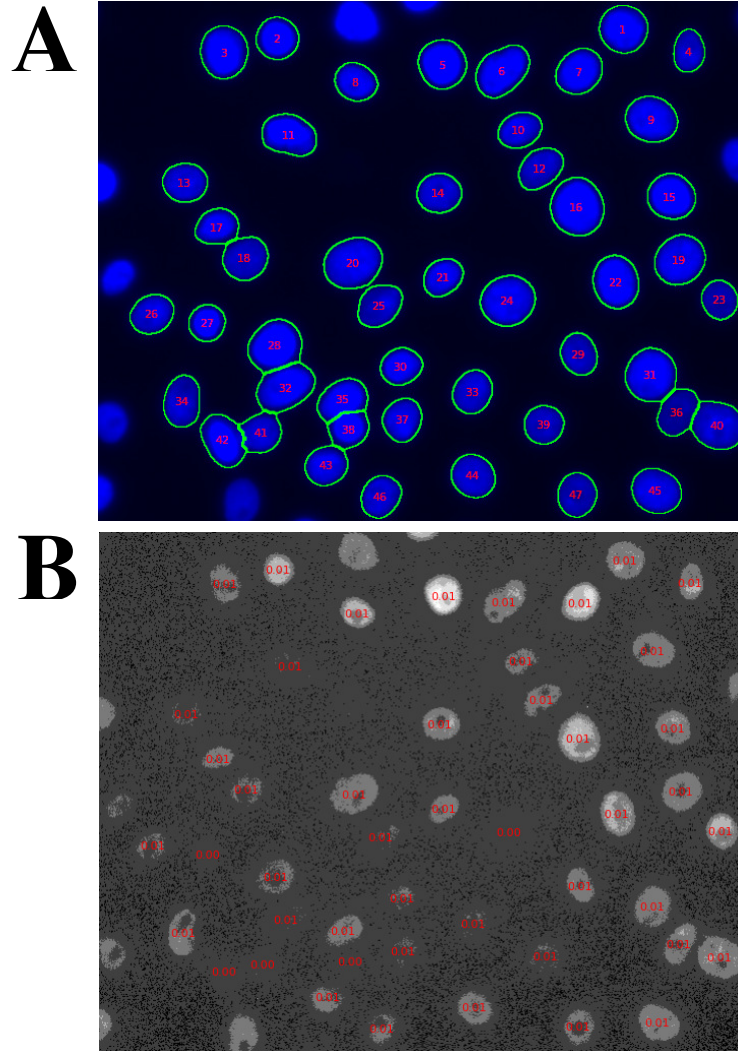
Figure 7. CellProfiler quantification of p53 positive cells. A) The number of nuclei is determined in the DAPI image and a mask is drawn around each nucleus. B) The image mask is overlaid on the corresponding p53 image and the mean red fluorescence intensity is quantified for each nucleus as well as for the background area not covered by nuclei. Nuclei with a mean red fluorescent intensity greater than the mean red background intensity plus three standard deviations were considered to be p53 positive.

2.8 Statistical Analyses

Statistical analyses and the creation of graphs were done using the open source programming language R, version 3.0.0 (R Development Core Team 2013). Data were determined to be parametric based on independence, normality and homogeneity of variance. Histograms, Q-Q plots and the Shapiro-Wilk's test were used to check normality. Bartlett's test was used to check homogeneity of variance. If normality was questionable, then the Levene's test was used. If required, data were transformed to regain parametric assumptions. Based on these results, one or two-way ANOVAs were used to determine global differences between the means. If significant differences were found, Tukey's HSD post hoc analyses were performed. The significance level (α) was set, *a priori*, at 0.05. Unless indicated otherwise, data represent mean +/- SEM.

3.0 RESULTS

3.1 EP and AA E6 Had Differing mRNA Structures

3.1.1 mRNA Secondary Structures

The secondary structure for each of the variant mRNAs was modeled to determine if the AA E6 SNPs resulted in changes which could have implications for the ability of the siRNA/RISC to access it. Due to the fact that the minimum free energy of an RNA molecule may not directly correspond to its actual biological conformation (Shapiro et al. 2007), the program CentroidFold which uses a centroid estimator was employed. Unlike programs such as RNAfold which choose the minimum free energy structure, CentroidFold creates an ensemble of secondary structures near the minimum free energy and then chooses the one which has the minimum number of predicted base pairs different from all others in the group to represent the sampled structures (Ding et al.

42

2005). The models generated by CentroidFold indicated that the secondary structures of the EP and AA E6 variants differed, due to the presence of the six SNPs in AA E6 (**Figure 8**). The AA variant mRNA appeared to have a more open structure in the area of the SNPs than that of the EP variant. Notably, this region corresponds to the portion of E6 which is spliced out of the truncated bicistronic transcripts in cells containing the full length viral genome, making it a favourable siRNA target.
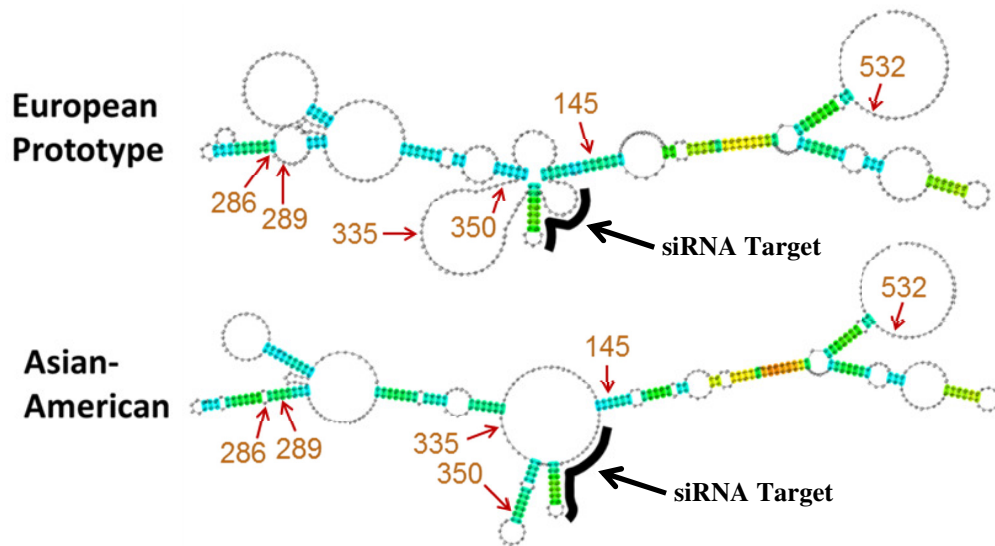
Figure 8. The mRNA secondary structures of the HPV16 EP and AA E6 variants (nt83-559). Modeling was done with the program CentroidFold. The six SNPs of the AA E6 variant resulted in it having a notably different structure than that of EP E6. The locations of the 6 SNPs are indicated with red arrows and the region of the transcript targeted by the E6 siRNA used in this study (nucleotides 386-404) is indicated by the thick black line. The colour gradation from blue to red corresponds to the probability between 0 to 1of the predicted hydrogen bond between two bases.

3.1.2 mRNA Tertiary Structures

To examine the three-dimensional structures created by the further folding of the above predicted mRNA secondary structures, 20 tertiary conformations were modeled favouring the base-pairings predicted by CentroidFold for each variant. Twenty possible conformations were chosen to provide a thorough sampling. The program FARNA was employed because it belongs to the well-established Rosetta software package which has been well referenced by a variety of independent groups (www.rosettacommons.org/publications). During the refinement of the predicted structures with molecular dynamics, the self-parameterizing Yamber force field, derived from the also well-known Amber force field (Krieger et al. 2004), was used for its suitability with biological molecules. **Table 3** shows each resulting possible conformation and the corresponding total free energy for each variant. The conformation with the most negative total free energy, -33 269 kcal/mol for EP E6 and -34 260 kcal/mol for AA E6, was chosen as the most probable tertiary mRNA structure for each variant. Both variants had similar total free energies. However, the AA E6 SNPs did also cause its tertiary mRNA structure to be different from that of EP E6 (**Figure 9**). It appeared that the AA E6 mRNA 3D structure was slightly less tightly compacted than that of the EP E6 mRNA.

Taken together, the results in section 3.1 showed that the secondary structure of the AA E6 variant was a more open loop than that of EP E6 in the region of the transcript targeted by the siRNA used in this study. In addition, the tertiary structure of the AA E6 mRNA appeared to not be as compact as that of EP E6. This lead to the inference that the

siRNA/RISC may be better able to access the AA E6 mRNA which would result in treatment with the same E6 siRNA having a higher knockdown efficacy in AA than EP E6. This was then tested in the subsequent *in vitro* experiments detailed below.

Table 3. Possible mRNA 3D conformations modeled for HPV16 E6 variants.

Variant	Conformation	Total Energy (kcal/mol)
EP E6	1	-30 710
EP E6	2	-12 850
EP E6	3	-7 426
EP E6	4	-22 204
EP E6	5	-30 225
EP E6	6	-3 965
EP E6	7	12 117
EP E6	8	-17 309
EP E6	9	-9 864
EP E6	10	-4 638
EP E6	11	-2 527
EP E6	12	-9 317
EP E6	13	10 959
EP E6	14	-12 872
EP E6	15	-21 650
EP E6	16	-16 413
EP E6	17	-27 710
EP E6	18	-33 269*
EP E6	19	-18 804
EP E6	20	-23 537
AA E6	1	-23 052
AA E6	2	-20 995
AA E6	3	-11 232
AA E6	4	18 510
AA E6	5	7 116
AA E6	6	-9 788
AA E6	7	-20 899
AA E6	8	-22 522
AA E6	9	-34 260*
AA E6	10	-14 049
AA E6	11	-22 972
AA E6	12	-18 183
AA E6	13	-12 052
AA E6	14	8 447
AA E6	15	-21 368
AA E6	16	-28 042
AA E6	17	5 667
AA E6	18	-16 158
AA E6	19	-17 758
AA E6	20	-29 080

*Most negative total energy and likely conformation.

European Prototype
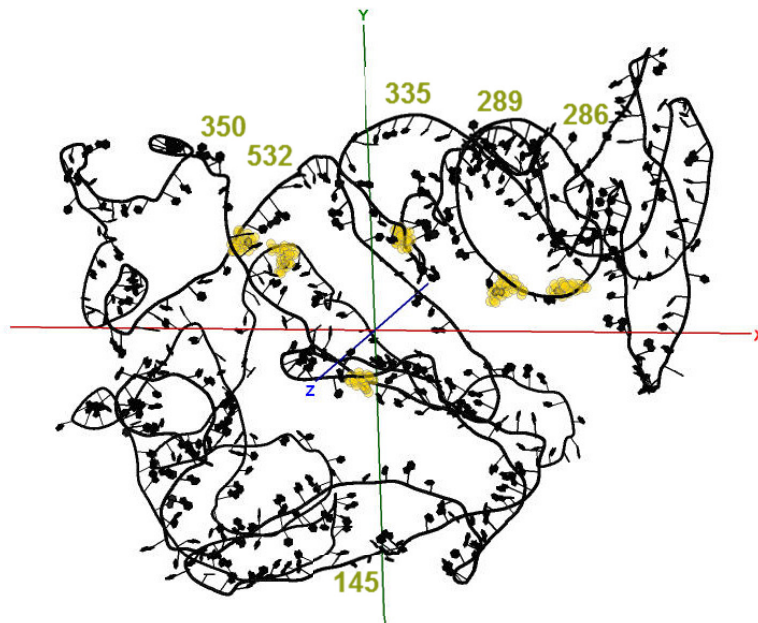
Asian-American
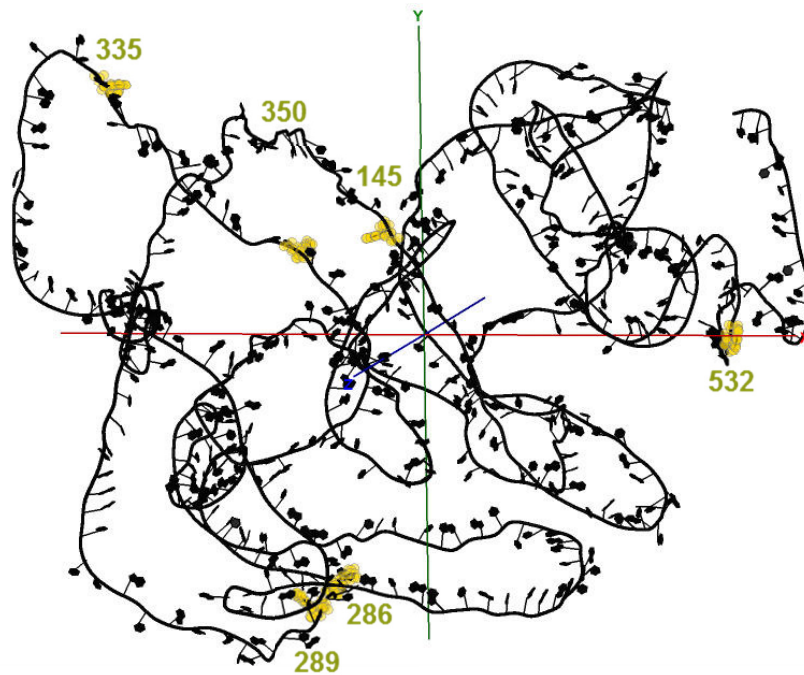
Figure 9. The mRNA tertiary structures of the HPV16 EP and AA E6 variants (nt83-559).

Images were rendered using the program Jmol. The six SNPs (highlighted in yellow) for the AA

E6 variant resulted in it having a different, slightly less compacted 3D structure than that of EP

E6.

3.2 PHFKs Transduced with EP or AA E6 Contained the Expected SNPs Following 30 Passages

The first step in a methodologically sound investigation is to verify the properties of the *in vitro* models being employed. In this instance, the cell culture model consisted of PHFKs which had been retrovirally transduced with either the EP or AA variant of HPV16 E6 by a previous graduate student in the lab, Sarah Niccoli, MSc (Niccoli et al. 2012). Over the two-year course of her study, these cells were followed for 30 passages through the processes of immortalization and malignant transformation induced by the presence of the viral E6 oncogene. These cells constitutively express E6 and were chosen over other HPV16 cell culture models, such as CaSki (Pattillo et al. 1977) and SiHa (Friedl et al. 1970), to avoid biases caused by HPV16 copy number differences (CaSki contains 200-600 and SiHa contains 1-2 genome copies of HPV16). Cells transfected with the full length variant genomes were not chosen either due to fluctuations in the ratio of episomal versus integrated HPV16 copies which can occur between passages (Robert Jackson, Thunder Bay Regional Research Institute; personal communication). Additionally, the use of these cells allowed us to study the differences in restoration of downstream cellular processes following suppression of EP and AA E6 without the influence of the other viral proteins.

Although highly unlikely, given the constant length of time that these cells were in culture for during the previous study it is always possible that some of the samples could have accidentally become mixed up with each other. This possibility could be refuted based on the following findings: At passage 30, both variants showed E6 DNA amplicons of the correct size (448 bp) following PCR (**Figure 10**). Positive (+) control

49

samples (Near-diploid Immortalized Keratinocytes (NIKS) (Allen-Hoffmann et al. 2000) transfected with the full length AA HPV16 genome) also showed the correct E6 DNA amplicons and no specific bands of E6 amplicon size were seen in the negative (-) control sample (PHFKs transduced with the HPV16 E7 gene only) or the H_2O sample. The sample of NIKS transfected with the AA HPV16 genome was kindly provided by current group member Robert Jackson, MSc and the PHFKs transduced with the E7 gene were the control cell line created by Niccoli et al. 2012. The consensus sequences obtained following Sanger sequencing of these amplicons confirmed that the SNPs (as described in Section 1.5) were located as expected, ensuring the findings in the subsequent sections were attributed to the correct variants.
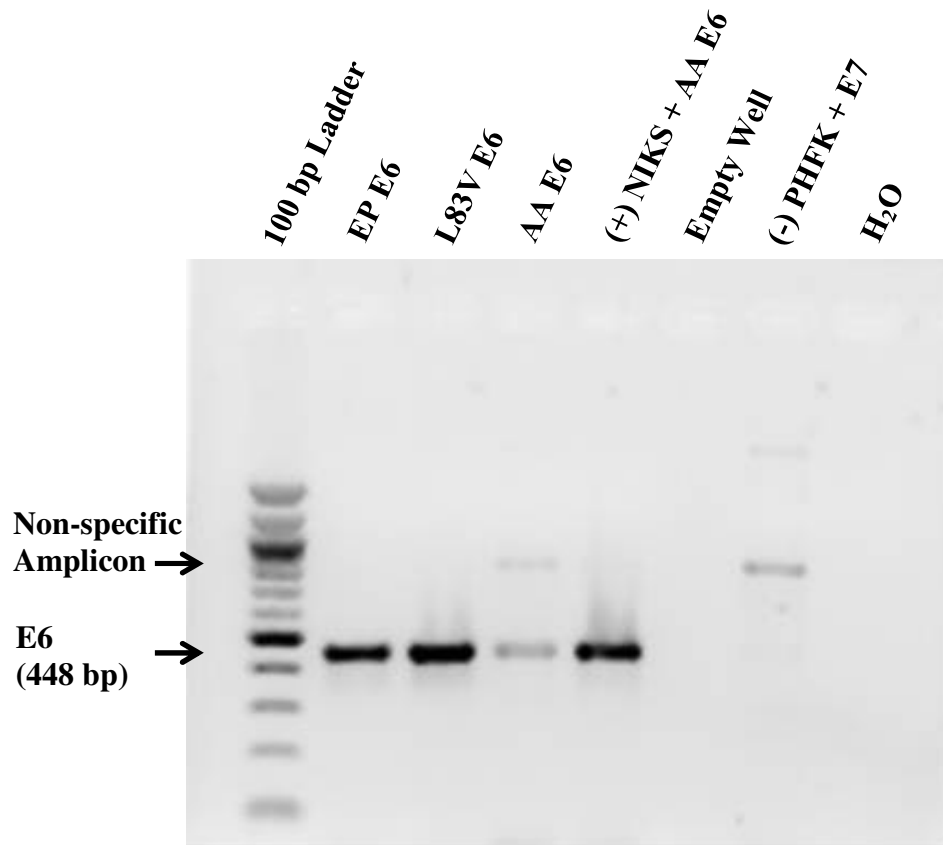
Figure 10. HPV16 E6 DNA PCR products. PCR products were separated on a 1.5% agarose gel. Both EP and AA E6 variants showed E6 amplicons of the correct size (448 bp), as well as the positive (+) control sample (Near–diploid Immortalized Kertatinocytes (NIKS) transfected with the full length AA HPV16 genome). No specific bands of E6 amplicon size were seen in the negative (-) control sample (PHFKs transduced with the HPV16 E7 gene only) or the H_2O sample. Due to the presence of a non-specific amplicon in the AA E6 sample, this band was excised from the gel and purified. The EP E6 PCR product was purified separately. This gel also contained the HPV16 L83V E6 variant which was not used in this study.

3.3 Relative mRNA Expression Changed Following Treatment with E6 siRNA

3.3.1 Both Variants Showed a Similar Knockdown of E6 mRNA

To determine whether the differing structures of the EP and AA E6 transcripts observed during the *in silico* modeling would be reflected in altered E6 siRNA knockdown efficacy between the variants, the cells were transfected with 10 and 25 nM of siRNA, respectively. These are siRNA concentrations near the lower end of the range found in the literature (Thakur et al. 2012 and references therein). Off-target effects from siRNA treatment can occur in two ways: 1) through the binding of the siRNA to other transcripts in the cell that it has near complete complementarity with (Thaker et al. 2012) and 2) through the binding of siRNA nucleotides 2-8 to the 3' untranslated regions of other transcripts (seed matching) (Birmingham et al. 2006). The use of as low a siRNA concentration as possible can help minimize these potential effects which may confound results. Untransduced PHFKs were used as a control because primary keratinocytes are the type of cells naturally infected with the HPV *in vivo* (zur Hausen et al. 2002). Forty-eight hours following transfection with 10 nM E6 siRNA, there was an 85.6% and 88.1% reduction in E6 expression compared to cells treated with scrambled siRNA for EP ($P <$ 0.001) and AA E6 ($P < 0.001$) respectively (**Figure 11A**). Interestingly, this difference in E6 knockdown between the two variants was not significantly different ($P = 0.929$). Similar results were obtained when the concentration of siRNA was increased to 25 nM, with EP E6 having a 90.4% reduction and AA E6 having an 89.1% reduction in E6 expression compared to cells treated with scrambled siRNA ($P < 0.001$ for both) (**Figure 11B**). Again, this difference in E6 knockdown between the variants was not significantly different ($P = 1.000$). The raw expression of E6 relative to HPRT1 in the baseline

medium only cells (8.06 for EP E6 and 8.22 for AA E6) (data not shown) was not significantly different between the variants, indicating that they both expressed similar starting levels of E6 mRNA. As expected, E6 expression was undetectable in all PHFK control samples. These findings were contrary to what was expected based upon the *in silico* modeling results. However, since E6 had been repressed to equivalent levels in both variants, comparison of the downstream response of cellular processes abrogated by E6 following treatment with E6 siRNA could then be studied for EP and AA E6.
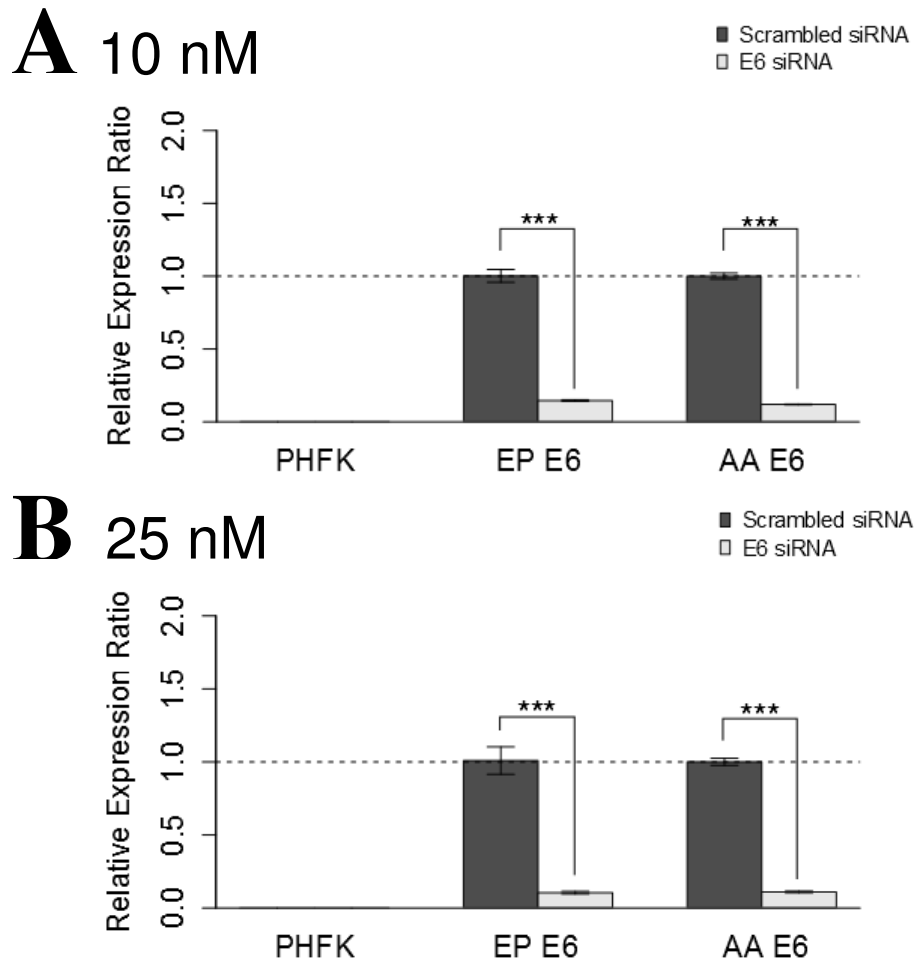
Figure 11. Relative E6 mRNA expression ratio following treatment with 10 or 25 nM siRNA. A) Treatment with 10 nM E6 siRNA significantly reduced E6 expression in both EP and AA E6 ($P < 0.001$ for both). The difference in E6 knockdown between the variants was not significant ($P = 0.929$). B) Treatment with 25 nM E6 siRNA significantly reduced E6 expression in both EP and AA E6 ($P < 0.001$ for both). The difference in E6 knockdown between the variants was not significant ($P = 1.000$). E6 was undetectable in PHFKs, as expected. Expression was determined relative to HPRT1 and calibrated to cells treated with scrambled siRNA. Statistical analysis was performed using a two-way ANOVA followed by Tukey's HSD contrasts post hoc. Data represent mean ± SEM, $n = 3$ for all. *** denotes $P < 0.001$.

3.3.2 hTERT Expression was Diminished to Normal Levels in AA but not in EP E6

The catalytic subunit of the enzyme telomerase, hTERT, is upregulated by the E6 proteins of high-risk *Alpha* papillomavirus types (Van Doorslaer and Burk 2012) and its expression plays a key role in immortalizing HPV16 infected cells (Klingelhutz et al. 1996, Gewin and Galloway 2001, Niccoli et al. 2012). Hence, this was the first cellular process downstream of E6 investigated. Treatment with 10 nM siRNA significantly diminished hTERT expression 86.8% and 95.5% compared to cells treated with scrambled siRNA, for EP E6 and AA E6 respectively ($P < 0.001$ for both) (**Figure 12A**). Although the difference in hTERT reduction between both variants was not significantly different ($P = 0.135$), treatment with E6 siRNA resulted in the hTERT level of AA E6 no longer being significantly different from that of PHFKs ($P = 0.688$) whereas the hTERT level of EP E6 remained significantly higher than that of PHFKs ($P = 0.012$). At the 25 nM siRNA concentration, treatment with E6 siRNA significantly diminished hTERT expression compared to cells treated with scrambled siRNA for both variants (83.7% and 93.7% for EP and AA E6 respectively, $P < 0.001$ for both) (**Figure 12B**). Again the difference in knockdown between both variants was not significant ($P = 0.179$) but AA E6 cells treated with E6 siRNA had a level of hTERT comparable to that of PHFKs ($P = 0.541$). The same was not true for EP E6 ($P = 0.010$). hTERT was mostly undetectable in all PHFK samples.

The raw expression of hTERT relative to HPRT1 (data not shown) was not significantly different between the variants in cells treated with 10 nM scrambled siRNA. However, in the cells treated with 25 nM scrambled siRNA, EP E6 had a higher level of hTERT than AA E6 ($P = 0.019$). This variable expression of hTERT has also been noted

by Niccoli et al. (2012). Still, it is interesting to note that when starting levels of hTERT are the same, treatment with the same dose of E6 siRNA still does not elicit an identical response in both variants.
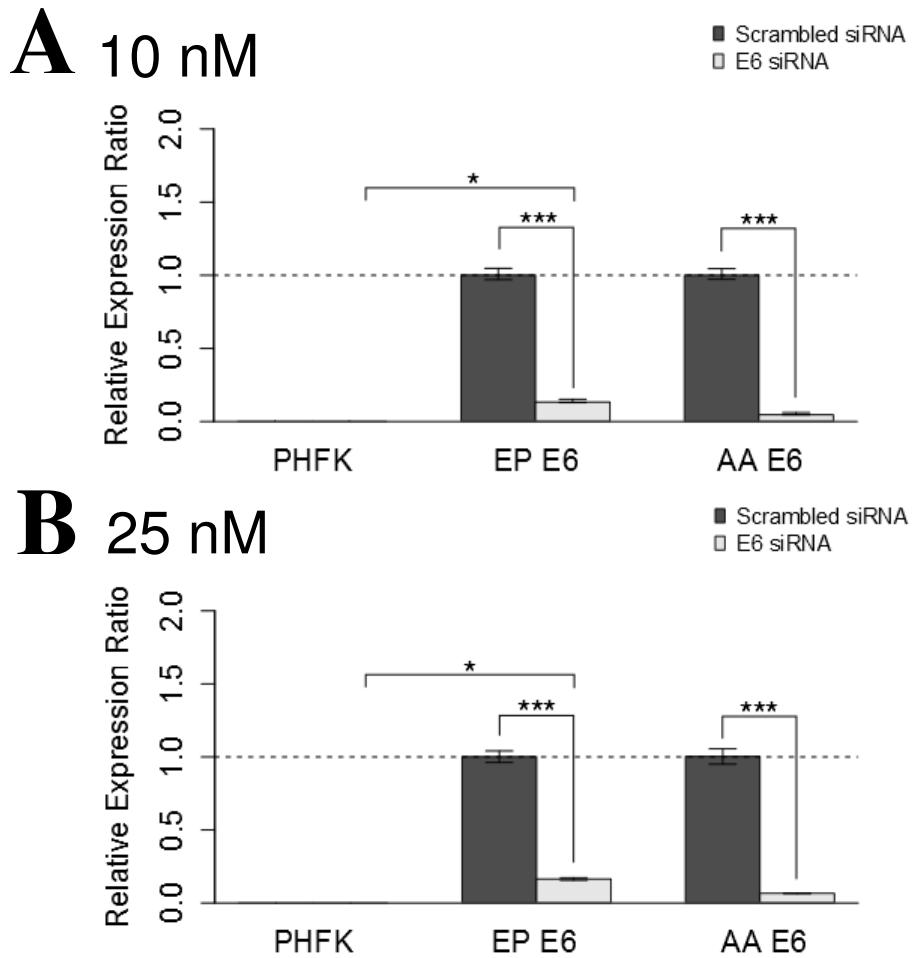
Figure 12. Relative hTERT mRNA expression ratio following treatment with 10 or 25 nM siRNA. A) Treatment with 10 nM E6 siRNA significantly reduced hTERT expression in both EP and AA E6 ($P < 0.001$ for both). AA E6 no longer had a significantly different hTERT expression than PHFKs ($P = 0.688$) but EP E6 did ($P = 0.012$). B) Treatment with 25 nM E6 siRNA significantly reduced hTERT expression in both EP and AA E6 ($P < 0.001$ for both). AA E6 no longer had a significantly different hTERT expression than PHFKs ($P = 0.541$) but EP E6 did ($P = 0.010$). Expression was determined relative to HPRT1 and calibrated to cells treated with scrambled siRNA. Statistical analysis was performed using a two-way ANOVA followed by Tukey's HSD contrasts post hoc. Data represent mean ± SEM, $n = 3$ for all. * denotes $P = 0.05$-0.01, *** denotes $P < 0.001$.

3.3.3 Expression of the Type I Interferons β and κ Differed Between the Variants

Activation of the innate immune system is a host's first line of defense against pathogens. It consists of various types of receptors, such as the Toll-like receptors, which become activated and lead to the induction of the Type I interferons, including IFN α and IFN β, and the Type II interferon, IFN γ (Koromilas et al. 2001), eliciting an adaptive immune response. Previous studies have shown HPV16 E6 is capable of binding to and deactivating interferon-regulatory factor 3 (IRF3) (Ronco et al. 1998), a transcriptional activator of Type I interferon production, and constitutively diminishing the levels of IFNs α and β mRNA within cervical keratinocytes retrovirally transduced with E6 or E6/E7 (Nees et al. 2001). Hence, the expression of IFN β in response to treatment with E6 siRNA was investigated here.

IFN β was Restored to Higher Levels in EP E6 Versus AA E6

Treatment with 10 nM siRNA resulted in a significant increase in IFN β expression regardless of cell type (P = 0.029) (**Figure 13A**). This increase in IFN β, which was also seen in PHFKs, was likely due to a non-specific response through activation of endosomal TLRs 7 and 8 or another cytosolic RNA sensor such as the RIG-I receptor by recognition of the siRNA (Kumar et al. 2011). At the 25 nM concentration, the E6 specific response became more evident. PHFK, EP E6 and AA E6 cells had 1.64, 4.51, and 1.85 fold increases in IFN β expression respectively and these were larger than the increases noted at the 10 nM concentration (**Figure 13B**). EP E6 cells treated with E6 siRNA had significantly more IFN β expression compared to cells treated with scrambled siRNA (P = 0.001). EP E6 cells treated with E6 siRNA also had significantly more IFN β expression compared to similarly treated AA E6 (P = 0.011) and PHFK cells (P = 0.006).
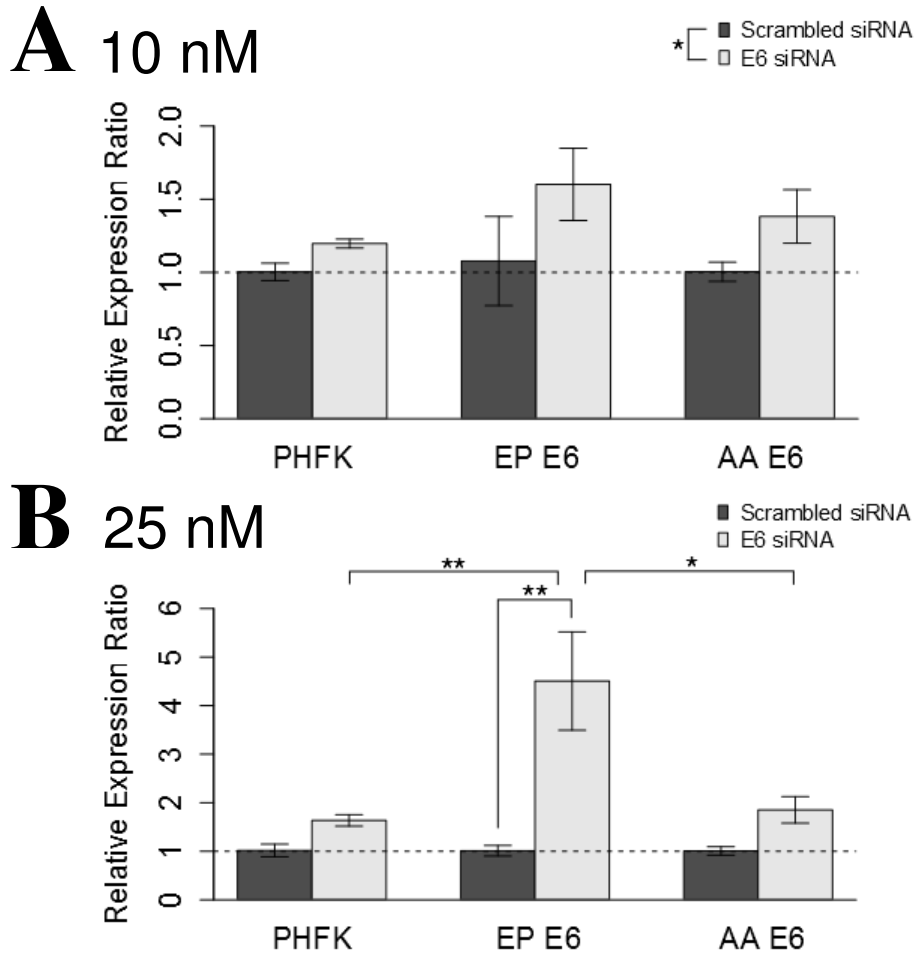
Figure 13. Relative IFN β mRNA expression ratio following treatment with 10 or 25 nM siRNA. A) Treatment with 10 nM E6 siRNA significantly increased IFN β expression, regardless of cell type ($P = 0.029$). B) Treatment with 25 nM E6 siRNA resulted in EP E6 having significantly increased IFN β expression compared to the corresponding PHFK and AA E6 cells ($P = 0.006$ and $P = 0.011$ respectively). Expression was determined relative to HPRT1 and calibrated to cells treated with scrambled siRNA. Statistical analysis was performed using a two-way ANOVA followed by Tukey's HSD contrasts post hoc. Data represent mean ± SEM, $n = 3$ for all. * denotes $P = 0.05$-0.01, ** denotes P = 0.01-0.001.

AA E6 IFN κ Expression was Elevated More by Treatment with a Lower siRNA Concentration than that of EP E6

IFN κ is a more recently discovered Type I interferon, which is expressed mainly in epidermal keratinocytes (LaFleur et al. 2001). IFN κ expression is repressed in HPV infected keratinocytes (Rincon-Orozoco et al. 2009, DeCarlo et al. 2010, Reiser et al. 2011). It has been suggested that the HPV16 E6 protein is responsible for this through p53 degradation and IFN κ DNA methylation (Rincon-Orozco et al. 2009, Reiser et al. 2011). After treatment with 10 nM siRNA, EP E6 had a significant 12.72 fold increase ($P < 0.001$) and AA E6 a significant 17.20 fold increase ($P < 0.001$) in IFN κ expression compared to cells treated with scrambled siRNA; whereas IFN κ expression remained unchanged in PHFKs ($P = 1.000$) (**Figure 14A**). IFN κ expression was restored significantly more in AA E6 than EP E6 ($P < 0.001$). After treatment with 25 nM siRNA, EP E6 had a significant 22.67 fold increase ($P < 0.001$) and AA E6 a significant 15.00 fold increase ($P = 0.022$) in IFN κ expression compared to cells treated with scrambled siRNA (**Figure 14B**). Again, IFN κ expression remained unchanged in PHFKs ($P = 1.00$). At this higher concentration, the increase in IFN κ expression is no longer significantly different between the variants ($P = 0.346$). As IFN κ expression remained unchanged in PHFKs, this seemed to be a more HPV16 E6 specific response than that of IFN β seen above.

IFN γ Expression Remained Undetectable

Since the Type II interferon, IFN γ, is downregulated in patient biopsies of malignant cervical lesions (de Gruijl et al. 1999), we wanted to investigate the potential

variant specific differences. However, its expression remained undetectable in all samples at both the 10 and 25 nM siRNA treatment concentrations.

It is also important to point out that, despite the large fold increases in IFN expression seen following treatment with E6 siRNA, their raw expression relative to HPRT1 (data not shown), particularly in the case of IFN κ, is still below that of untransduced PHFKs. This is not clearly evident from the way the expression data is presented above.
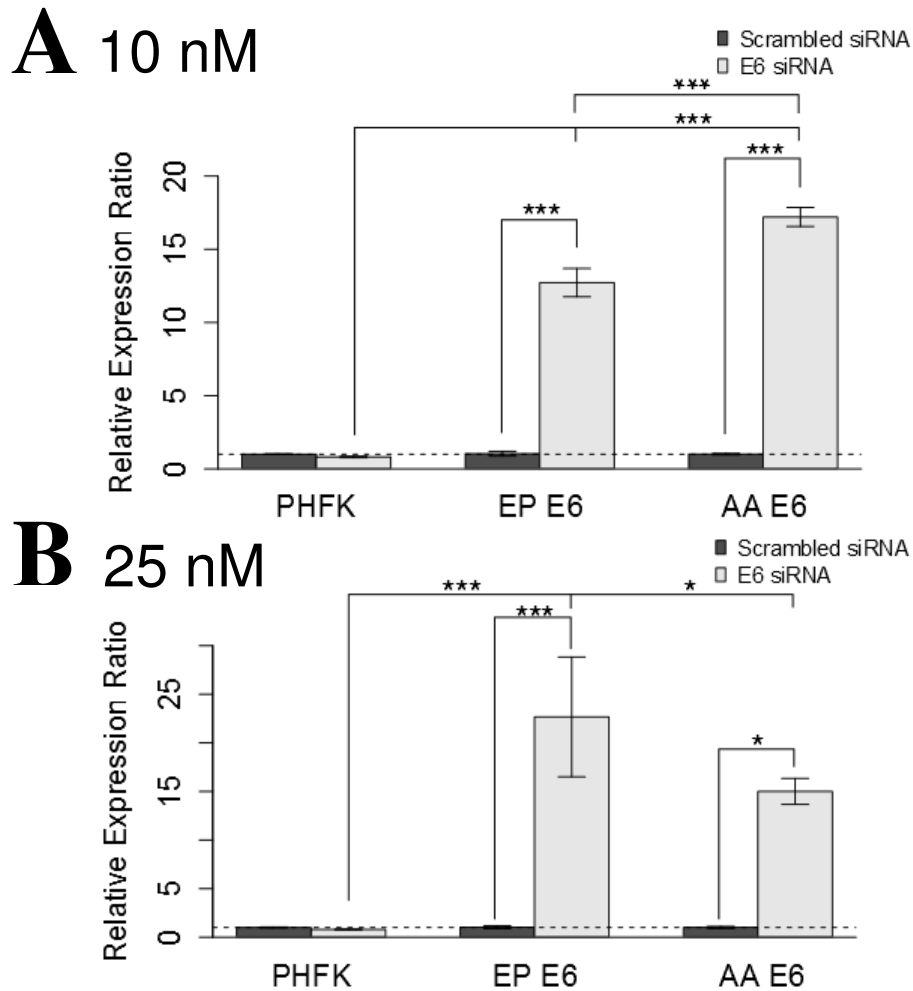
Figure 14. Relative IFN κ mRNA expression ratio following treatment with 10 or 25 nM siRNA. A) Treatment with 10 nM E6 siRNA significantly increased IFN κ expression in EP and AA E6 ($P < 0.001$ for both). The increase in IFN κ expression was significantly greater in AA E6 than EP E6 ($P < 0.001$). B) Treatment with 25 nM E6 siRNA significantly increased IFN κ expression in EP and AA E6 ($P < 0.001$ and $P = 0.022$ respectively). The difference in the increase of IFN κ expression between the variants was no longer significant ($P = 0.346$). Expression was determined relative to HPRT1 and calibrated to cells treated with scrambled siRNA. Statistical analysis was performed using a two-way ANOVA followed by Tukey's HSD contrasts post hoc. Data represent mean ± SEM, $n = 3$ for all. * denotes $P = 0.05$-0.01, *** denotes $P < 0.001$.

3.4 E6 Expression was Also Diminished at the Protein Level Following Treatment With E6 siRNA

There is not always a direct one-to-one relationship between the amount of a transcript and the corresponding amount of protein within a cell (Gry et al. 2009). Because the E6 siRNA resulted in an equal knockdown of E6 mRNA for both variants, E6 expression was then examined at the protein level to see if a similar pattern was continued and to provide further insight into the differences observed above in the restoration of cellular processes downstream of E6. Indirect detection of the E6 protein using antibodies is challenging, due to the fact that E6 is a small (18 kDa) protein with many binding partners (Jackson et al. 2013). Also, the E6 mouse monoclonal antibody, which produces the most reliable results (clone 4C6; Arbor Vita Corporation, Fremont, CA, USA), is not commercially available. Hence, a Western blot was done to detect the human influenza hemagglutinin (HA) tag located on the transduced E6 protein. This approach is also beneficial because it eliminates any potential detection biases which could be caused if the E6 antibody had different binding affinities for each of the E6 variants. The Western blot indicated that treatment with 10 and 25 nM E6 siRNA, respectively both resulted in elimination of a detectable amount of protein for EP and AA E6 (**Figure 15**). Unfortunately, this meant that no comparison of E6 protein expression between these particular variant samples could be made. As expected, the E6-HA protein was not detectable in any of the PHFK samples. No non-specific bands were present on the membrane.
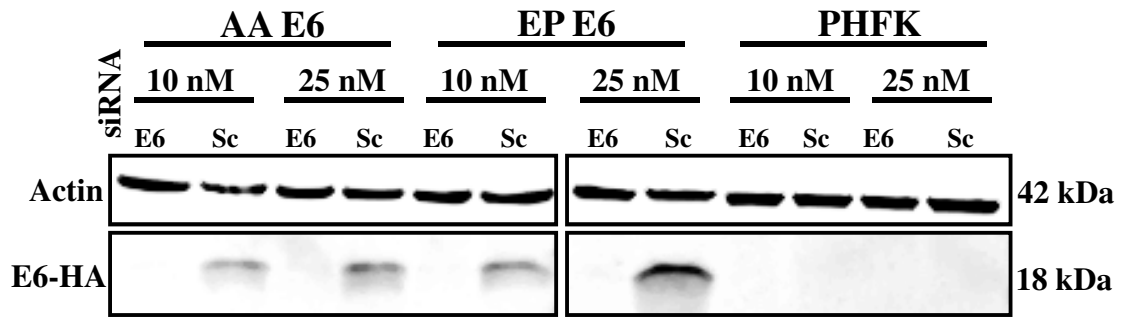
Figure 15. Western blot for the E6 protein HA tag following treatment with 10 or 25 nM siRNA. Treatment with both concentrations of E6 siRNA reduced the E6-HA protein below detectable limits for both EP and AA E6. No bands were detected for PHFKs, as expected. $n = 1$.

3.5 AA E6 p53 Protein Expression was Restored by Treatment with a Lower siRNA Concentration than that Required by EP E6

Since E6-HA expression could not be compared directly between EP and AA E6 using a Western blot due to the observed detection limit issues, p53 protein levels were then investigated to help gain a better understanding of what was happening to E6 at the protein level. Quantitative immunofluorescence, a powerful technique previously employed by our group in a similar manner (Togtema et al. 2012), was used to determine the percentage of cells positive for p53 staining, an indicator of diminished E6 protein levels (**Figure 16**). Treatment with 10 nM E6 siRNA resulted in significantly more p53 positive cells than treatment with the scrambled siRNA, the transfection reagent only, or medium only for EP E6 ($P < 0.001$ for all) (**Figure 17A**). The same comparisons were noted for AA E6 ($P < 0.001$ for all). EP E6 treated with E6 siRNA had a significantly lower percentage of p53 positive cells than both AA E6 and PHFKs treated with E6 siRNA ($P < 0.001$ for both). AA E6 cells treated with E6 siRNA had a p53 level restored to that of the PHFKs ($P = 0.999$). Treatment with 25 nM E6 siRNA also resulted in significantly more p53 positive cells than treatment with scrambled siRNA, the transfection reagent only, or medium only for both EP and AA E6 ($P < 0.001$ for all) (**Figure 17B**). At this higher siRNA concentration, the p53 levels of both EP and AA E6 were no longer significantly different from that of PHFKs ($P = 0.504$ and $P = 1.000$ respectively). There was a slight non-specific stress response to the transfection reagent and siRNAs in the PHFKs, as evidenced by an increase in p53 expression compared to cells treated with medium only. These results suggested that AA E6 cells treated with E6 siRNA may have had lower levels of E6 protein than the corresponding EP E6 cells.

Another possibility is that the E6 protein levels were not that different between the variants, but that EP E6 differs in the mechanism by which it leads the degradation of p53 or its ability to do so, compared to AA E6.
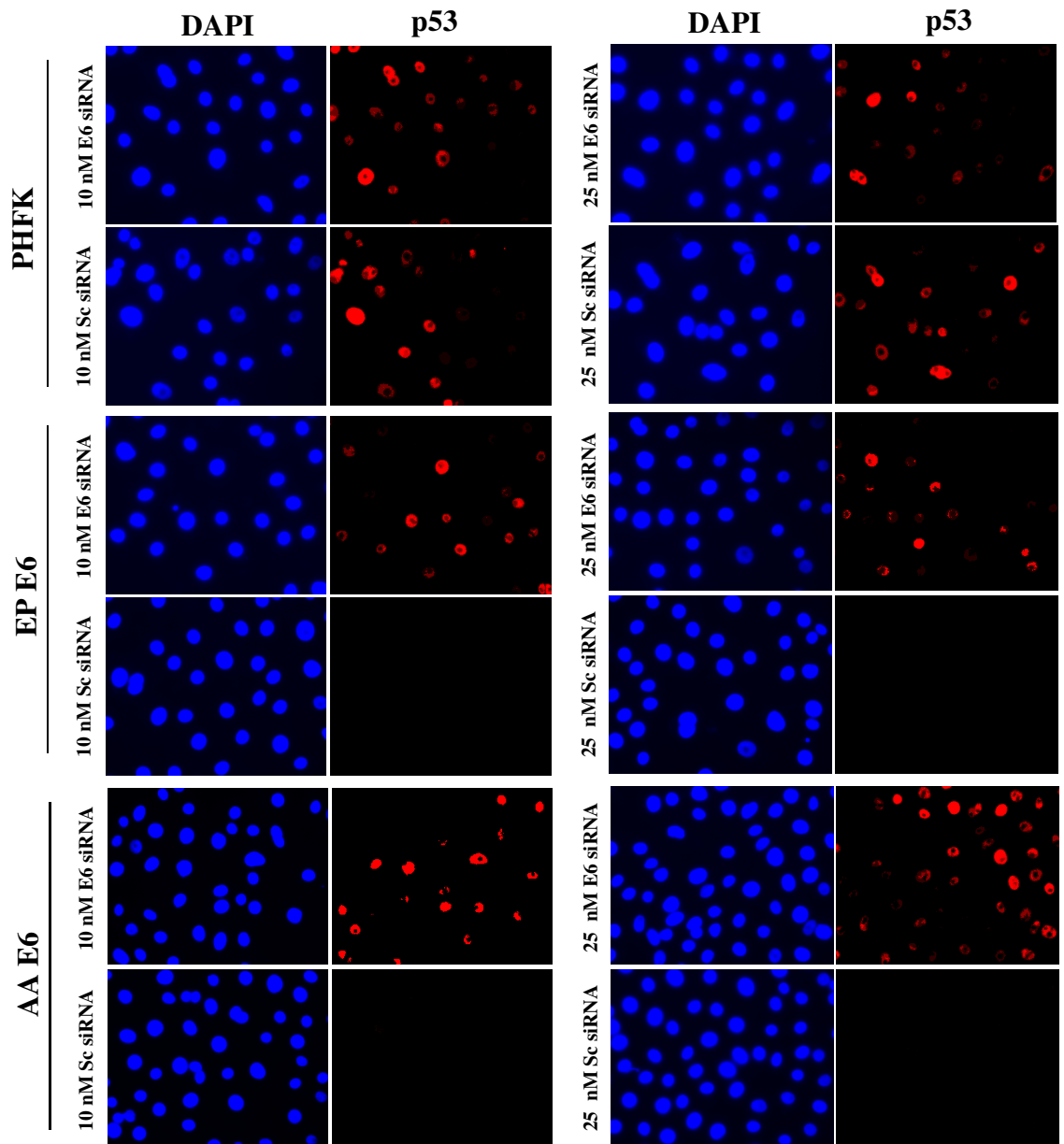
Figure 16. Immunofluorescent detection of p53 positive cells following treatment with 10 or 25 nM siRNA. p53 expression (red) is restored following treatment with E6 siRNA and is mostly undetectable following treatment with scrambled siRNA for both EP and AA E6. p53 expression is detectable in both PHFKs treated with E6 or scrambled siRNA. Nuclei were counterstained with DAPI (blue).
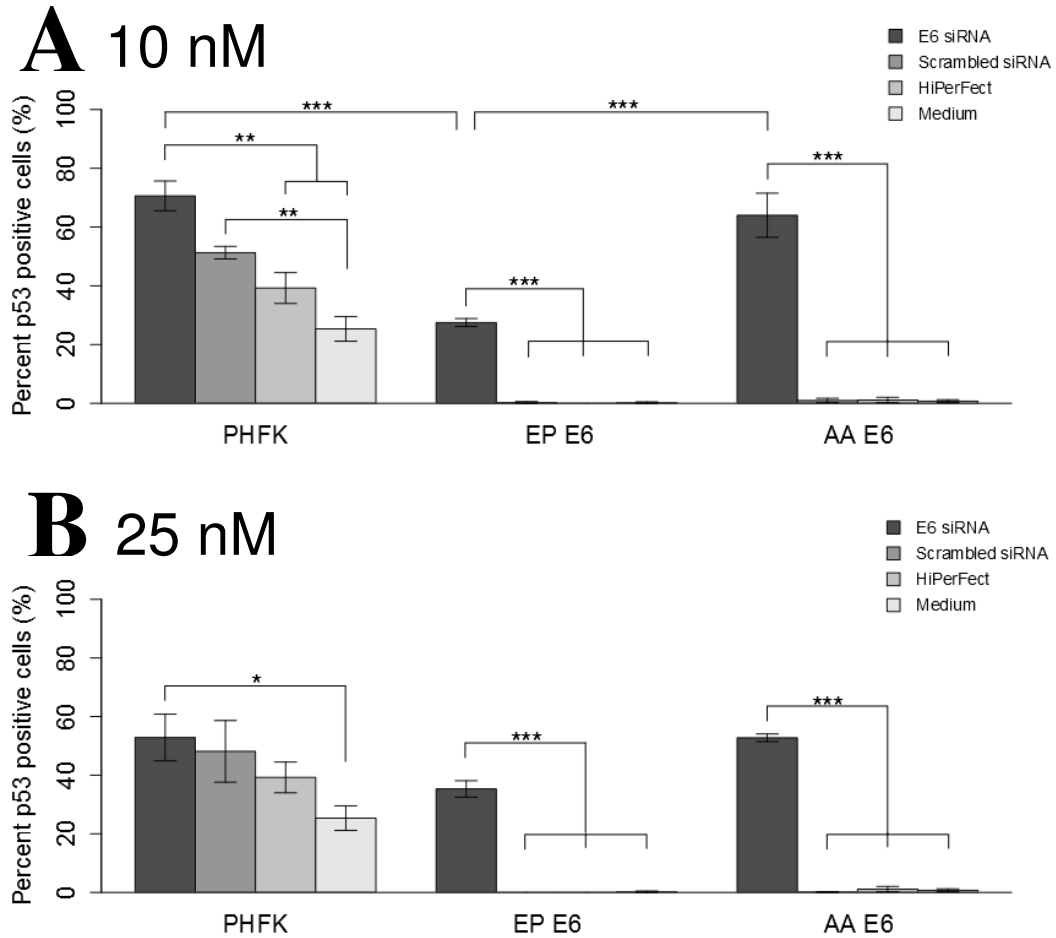
Figure 17. p53 protein expression following treatment with 10 or 25 nM siRNA. Data were transformed using a square root transformation. A) Treatment with 10 nM E6 siRNA significantly restored p53 expression in EP and AA E6 compared to controls ($P < 0.001$ for all). p53 expression was still significantly lower in E6 siRNA treated EP E6 than PHFK and AA E6 ($P < 0.001$ for both). B) Treatment with 25 nM E6 siRNA significantly restored p53 expression in EP and AA E6 compared to controls ($P < 0.001$ for all). p53 expression in PHFK, EP E6, and AA E6 cells treated with E6 siRNA were no longer different from each other. Statistical analysis was performed using a two-way ANOVA followed by Tukey's HSD contrasts post hoc. Data represent mean ± SEM, $n = 3$ for all. * denotes $P = 0.05\text{-}0.01$, ** denotes $P = 0.01\text{-}0.001$, and *** denotes $P < 0.001$.

4 DISCUSSION

4.1 Comparison of the E6 mRNA Structural Model Predictions to Experimental E6 siRNA Knockdown Efficacy for the Variants

The *in silico* models predicted for the variant mRNAs demonstrated that the six SNPs present in AA E6 altered both its secondary and tertiary structures compared to EP E6. AA E6 had a more open loop secondary structure in the area targeted by the E6 siRNA and a less tightly compact 3D structure. These observations led us to infer that the AA E6 transcript would be more accessible for the siRNA/RISC and that the same E6 siRNA would have a higher E6 knockdown efficacy for AA than EP E6. However, this was not confirmed by the results of our *in vitro* experiments. Both variants showed an equal knockdown in the expression of E6 mRNA compared to cells treated with scrambled siRNA and this was noted following treatment with both 10 and 25 nM E6 siRNA respectively.

This discrepancy can be the result of several factors. First, it is possible that our *in silico* models may not accurately represent the true structure of the variant E6 mRNAs. Modeling of a single RNA molecule is a complex process and predictions are hampered by minimal knowledge of the thermodynamic properties of complex structural elements such as pseudoknots (Shapiro et al. 2007), which may be present. Comparative approaches, which take into account the determined structures for homologous sequences and search for a consensus between them may be provide a more accurate prediction (Rivas 2013). Although costly and labour intensive, further improvement of experimental techniques including x-ray crystallography and nuclear magnetic resonance (NMR) are also needed to accurately provide important atomic level structural details (Shapiro et al.

2007). Secondly, it is possible that our structural models are comparable to the naïve structures of the E6 variant mRNAs but that the differences observed are not of a large enough magnitude to significantly impair access of the RISC/siRNA. Only one E6 siRNA was employed in this study and it would be worthwhile to investigate whether additional sequences targeting other locations of the transcript predicted to be structurally different between the variants in our model would yield results similar to those obtained here.

4.2 Differential Restoration of Downstream Cellular Processes Abrogated by HPV16 E6

Following the knockdown of E6 mRNA to statistically similar levels in both variants, it was then possible to study the differences in the restoration of downstream cellular processes abrogated by the E6 protein between EP and AA E6. Treatment with E6 siRNA resulted in the restoration of hTERT mRNA levels to those of PHFKs in AA E6. Within the innate immune system pathways, treatment with E6 siRNA resulted in a greater elevation of IFN β mRNA expression in EP compared to AA E6. AA E6 IFN κ mRNA expression was elevated more following treatment with a lower dose of E6 siRNA than that of EP E6 and this corresponded to the restoration of AA E6 p53 protein levels following treatment with a lower concentration of E6 siRNA than that required by EP. These data provide evidence supporting the existence of a positive feedback loop between IFN κ transcript and p53 levels which is required for an effective innate immune response in keratinocytes, as reported by Rincon-Orozco et al. (2009).

The occurrence of these differences despite equivalent E6 transcript levels remaining in AA and EP E6 cells following treatment with E6 siRNA is an interesting

finding. One possible explanation is that the corresponding E6 protein levels may instead be different between the variants, which unfortunately could not be confirmed in this study. A recent high-throughput, genome wide study in yeast (*S. cerevisiae*) has found that transcripts with weakly folded 5'-untranslated region (UTR) secondary structures have longer half-lives, higher translation rates and higher resulting protein abundances than transcripts with strongly folded 5'-UTR secondary structures (Ringnér and Krogh 2005). A similar such mechanism could potentially alter E6 mRNA translation between AA and EP E6. However, in the study completed by Niccoli et al. (2012), HA Western blots done on these same cells but untreated with siRNA showed no significant difference in E6-HA expression between EP and AA E6.

Another possibility, and which is suggested by the similar mRNA knockdown of both E6s, is that the corresponding E6 protein levels following treatment with E6 siRNA are not different between the variants but that AA E6 interacts with other molecules in the cell or disrupts cellular processes differently than EP E6. For example, together with c-myc the E6/E6AP complex of high-risk HPV types binds to E-box elements within the hTERT promoter, up regulating hTERT expression (Veldman et al. 2003, Van Doorslaer and Burk 2012). It is possible that EP E6 has a different binding affinity for the E-box promoter elements than AA E6. Other mechanisms have also been implicated in E6's ability to upregulate hTERT transcription. It has been reported that the E6/E6AP complex can bind to and degrade the NFX1-91 transcriptional repressor of hTERT (Gewin et al. 2004). As well, the E6/E6AP complex has also been reported to bind NFX1-123, a transcriptional activator of hTERT, helping recruit it to the promoter (Katzenellenbogen et al. 2007) and it has been suggested that E6 may still be able to achieve this even in the

71

absence of E6AP (Sekaric et al. 2008). Perhaps the variants employ different combinations of these mechanisms.

4.3 Difference in E6 Knockdown Between Treatment with 10 or 25 nM E6 siRNA

Another interesting finding was that treatment of the cells with 10 nM E6 siRNA resulted in an average knockdown of ~87% of E6 transcript expression. However, increasing the siRNA dose 2.5x to 25 nM only resulted in a slight increase, at an average knockdown of ~89.8%. It was suspected that this may be related to the short half-life and stability of the siRNA once transfected into cells (Corey 2007, Dutta et al. 2011b). Hence, 2'-OMe nucleotides were added to the E6 siRNA sequence in four different patterns (**Appendix 7**). 2'-OMe nucleotides contain the substitution of an O-methyl (OMe) for the hydroxyl group (OH) on the 2' carbon of the ribose ring of the nucleotide and have been shown to increase siRNA stability and efficacy (Shukla et al. 2010). However, none of the modification patterns resulted in significantly more E6 suppression than the unmodified siRNA.

Micro-RNAs (miRNAs), another class of endogenous, small non-coding RNAs commonly involved in gene expression regulation (Kaczkowski et al. 2012), also function through the shared usage of some of the same cellular machinery as siRNAs. Pre-miRNAs formed in the nucleus are carried out into the cytoplasm where they are also cleaved by Dicer into active miRNAs (Shukla et al. 2010). The miRNAs are then picked up by Argonaute 2 and other proteins, forming the miRISC which cleaves the target transcript if the miRNA has perfect complementarity to it or acts to stall translation if there is incomplete complementarity (Shukla et al. 2010). Over 1 048 endogenous miRNAs have been identified in humans (Kaczkowski et al. 2012). The normal

processing of these miRNAs coupled together with the introduction of exogenous, synthetic siRNA may saturate the machinery of the RNAi pathway, rendering a larger dose of siRNA ineffective.

5 CONCLUSIONS AND FUTURE DIRECTIONS

To our knowledge, this was the first study to explore the potential changes that the six AA SNPs may have on the secondary and tertiary structures of the E6 mRNA as well as to compare in detail the differences in E6 silencing and the restoration of cellular processes abrogated by E6 for each variant in a post-integrative scenario. These findings fit well with those of another current project in the group which show that the EP and AA E6 variants differ in their abilities to initiate early carcinogenesis, in an early infection scenario with the full-length viral genome (Robert Jackson, Thunder Bay Regional Research Institute; personal communication). Future studies now need to elucidate the mechanisms underlying these observations and whether they are related to altered binding abilities of the E6 protein or differences in the way cellular processes are disrupted for each of the variants. Reconfirmation that the protein levels of EP and AA E6 do not differ, as reported by Niccoli et al. 2012, should be evaluated. Further optimization of the HA western blot and the use of high-throughput techniques, such as RNA sequencing (Wang et al. 2009), may aid in answering these questions. Difficulties in experimentally modeling the structure of the full E6 protein using NMR have only recently been overcome (Zanier et al. 2012). Future experimental determination of the structures of the EP and AA E6 proteins in a similar manner would provide useful additional information. It is also needed to determine whether similar differences will persist in the context of the full length HPV16 genome E6/E7 bicistronic transcript and

the presence of the other viral proteins. Although DAPI stained nuclei observed while collecting the p53 data did not show evidence of a notable increase in apoptotic cells, experiments are also currently in progress to evaluate cleaved Poly(ADP-ribose) polymerase-1 (PARP) staining, an early marker of apoptosis (Soldani and Scovassi 2002), in each variant following treatment with 10 or 25 nM of this E6 siRNA. As well, experiments are also currently underway to confirm whether transfection of EP E6 with the 2'-OMe modified E6 siRNAs yields similar results to those obtained here with AA E6. Other modifications, such as carba-locked nucleic acids (Dutta et al. 2011a), may yield more successful increases in siRNA efficacy

These findings may eventually lead to a translational impact. Genotyping can be employed to determine which variant of HPV16 a patient is infected with. Knowing this, higher doses of E6 siRNA or an siRNA containing an immune stimulatory motif may need to be given to those infected with the EP E6 variant to obtain the same restoration of IFN κ and p53 expression, key players in initiating an innate immune response and apoptosis, as possibly obtained with lower doses in patients infected with AA E6. One of the hurdles to translation will be safe and efficient delivery of the therapeutic siRNAs. In addition to chemical modification for the improvement of siRNA stability, packaging of the siRNA into liposomes or nanoparticles can also add protection and improve cellular uptake (Wang et al. 2011). Localised, topical application of the siRNA to cervical lesions may potentially require lower doses and cause less unwanted immunogenic effects than those associated with systemic delivery (Singhania et al. 2012), making lower grade CINs a more plausible target for early clinical trials than invasive carcinoma.

6 REFERENCES

Allen-Hoffman, B. L., Schlosser, S. J., Ivarie, C. A., Sattler, C. A., Meisner, L. F., O'Connor, S. L., 2000. Normal growth and differentiation in a spontaneously immortalized near-diploid human keratinocyte cell line, NIKS. J. Invest. Dermatol. 114, 444-455.

Bernard, H. U., Burk, R. D., Chen, Z., van Doorslaer, K., zur Hausen, H., de Villiers, E. M., 2010. Classification of papillomaviruses (PVs) based on 189 PV types and proposal of taxonomic amendments. Virology 401, 70-79.

Berumen, J., Ordoñez, R. M., Lazcano, E., Salmeron, J., Galvan, S. C., Estrada, R. A., Yunes, E., Garcia-Carranca, A., Gonzalez-Lira, G., Madrigal-de la Campa, A., 2001. Asian-American variants of human papillomavirus 16 and risk for cervical cancer: a case-control study. J. Natl. Cancer Inst. 93, 1325-1330.

Birmingham, A., Anderson, E. M., Reynolds, A., Ilsley-Tyree, D., Leake, D., Fedorov, Y., Baskerville, S., Maksimova, E., Robinson, K., Karpilow, J., Marshall, W. S., Khvorova, A., 2006. 3' UTR seed matches, but not overall identity, are associated with RNAi off-targets. Nat. Methods 3, 199-204.

Bohula, E. A., Salsibury, A. J., Sohail, M., Playford, M. P., Riedemann, J., Southern, E. M., Macaulay, V. M., 2003. The efficacy of small interfering RNAs targeted to the type 1 insulin-like growth factor receptor (IGF1R) is influenced by secondary structure in the IGF1R transcript. J. Biol. Chem. 278, 15991-15997.

Boshart M., Gissmann, L., Ikenberg, H., Kleinheinz, A., Scheurlen, W., zur Hausen, H., 1984. A new type of papillomavirus DNA, its presence in genital cancer biopsies and in cell lines derived from cervical cancer. EMBO J. 3, 1151-1157.

75

Buckley, C. H., Butler, E. B., Fox, H., 1982. Cervical intraepithelial neoplasia. J. Clin. Pathol. 35, 1-13.

Butz, K., Ristriani, T., Hengstermann, A., Denk, C., Scheffner, M., Hoppe-Seyler, F., 2003. siRNA targeting of the viral E6 oncogene efficiently kills human papillomavirus-positive cancer cells. Oncogene 22, 5938-5945.

Courtête, J., Sibler, A. P., Zeder-Lutz, G., Dalkara, D., Oulad-Abdelghani, M., Zuber, G., Weiss, E., 2007. Suppression of cervical carcinoma cell growth by intracytoplasmic codelivery of anti-oncoprotein E6 antibody and small interfering RNA. Mol. Cancer Ther. 6, 1728-1735.

Carpenter, A. E., 2007. Software opens the door to quantitative imaging. Nat. Methods 4, 120-121.

Carpenter, A., E., Jones, T. R., Lamprecht, M. R., Clarke, C., Kang, I. H., Friman, O., Guertin, D. A., Chang, J. H., Lindquist, R. A., Moffat, J., Golland, P., Sabatini, D. M., 2006. CellProfiler: image analysis software for identifying and quantifying cell phenotypes. Genome Biol. 7, R100.

Corey, D. R., Chemical modification: the key to clinical application of the RNA interference? J. Clin. Invest. 117, 3615-3622.

Cristofari, G., Darlix, J. L., 2002. The ubiquitous nature of RNA chaperone proteins. Prog. Nucleic Acid Res. Mol. Biol. 72, 223-268.

Crow, J. M., 2012. HPV: the global burden. Nature 488, S2-S3.

Daling, J. R., Madeleine, M. M., Johnson, L. G., Schwartz, S. M., Shera, K. A., Wurscher, M. A., Carter, J. J., Porter, P. L., Galloway, D. A., McDougall, J. K.,

2004. Human papillomavirus, smoking, and sexual practices in the ethiology of anal cancer. Cancer 101, 270-280.

Das, R., Baker, D., 2007. Automated de novo prediction of native-like RNA tertiary structures. Proc. Natl. Acad. Sci. USA 104, 14664-14669.

DeCarlo, C. A., Escott, N. G., Werner, J., Robinson, K., Lambert, P. F., Law, R. D., Zehbe, I., 2008. Gene expressioni analysis of interferon kappa in laser capture microdissected cervical epithelium. Anal. Biochem. 381, 59-66.

DeCarlo, C. A., Severini, A., Edler, L., Escott, N. G., Lambert, P. F., Ulanova, M., Zehbe, I., 2010. IFN-κ, a novel type I IFN, is undetectable in HPV-positive human cervical keratinocytes. Lab Invest. 90, 1482-1491.

de Gruijl, T. D., Bontkes, H. J., van den Muysenberg, A. J., van Oostveen,, J. W., Stukart, M.J., Verheijen, R. H. van der Vange, N., Snijders, P. J., Meijer, C.J., Walboomers, J. M., Scheper, R. J., 1999. Differences in cytokine mRNA profiles between premalignant and malignant lesions of the uterine cervix. Eur. J. Cancer 35, 490-497.

de Villiers, E. M., Fauquet, C., Broker, T. R., Bernard H. U., zur Hausen, H., 2004. Classification of papillomaviruses. Virology 324, 17-27.

Ding, Y., Chan, C. Y., Lawrence, C. E., 2005. RNA secondary structure prediction by centroids in a Boltzmann weighted ensemble. RNA 11, 1157-1166.

Doorbar, J., 2005. The papillomavirus life cycle. J. Clin. Virol. 32, S7-S15.

Doorbar, J., Quint, W., Banks, L., Bravo, I. G., Stoler, M., Broker, T. R., Stanley, M. A., 2012. The biology and life-cycle of human papillomaviruses. Vaccine 30S, F55-F70.

Dürst, M., Gissmann, L., Ikenberg, H., zur Hausen, H., 1983. A papillomavirus DNA from a cervical carcinoma and its prevalence in cancer biopsy samples from different geographic regions. Proc. Natl. Acad. Sci. USA 80, 3812-3815.

Dutta, S., Bhaduri, N., Rastgoi, N., Chandel, S. G., Vandavasi, J. K., Upadhayaya, R. S., Chattopahyaya, J., 2011a. Carba-LNA modified siRNAs targeting HIV-1 TAR region downregulate HIV-1 replication successfully with enhanced potency. Med. Chem. Commun. 2, 206-216.

Dutta, S., Bhaduri, N., Upadhayaya, R. S., Rastogi, N., Chandel, S. G., Vandavasi, J. K., Plashkevych, O., Kardile, R. A., Chattopadhyaya, J., 2011b. The R-diastereomer of 6'-O-toluoyl-carba-LNA modification in the core region of siRNA leads to 24-times improved RNA silencing potency against the HIV-1 compared to its S-counterpart. Med. Chem. Commun. 2, 1110-1119.

Elbashir, S. M., Harborth, J., Lendeckel, W., Yalcin, A., Weber, K., Tuschl, T., 2001. Duplexes of 21-nucleotide RNAs mediate RNA interference in cultured mammalian cells. Nature 411, 494-498.

Fire, A., Xu, S., Montgomery, M. K., Kostas, S. A., Driver, S. E., Mello, C. C., 1998. Potent and specific genetic interference by double-stranded RNA in Caenorhabditis elegans. Nature 391, 806-811.

Forman, D., de Martel, C., Lacey, C. J., Soerjomataram, I., Lortet-Tieulent, J., Bruni, L., Vignat, J., Ferlay, J., Bray, F., Plummer, M., Franceschi, S., 2012. Global burden of human papillomavirus and related diseases. Vaccine 30S, F12-F23.

Friedl, F., Kimura, I., Osato, T., Ito, Y., 1970. Studies on a new human cell line (SiHa) derived from carcinoma of uterus. I. Its establishment and morphology. Proc. Soc. Exp. Bio. Med. 135, 543-545.

Gardiol, D., Kuhne, C., Glaunsinger, B., Lee, S. S., Javier, R., Banks. L., 1999. Oncogenic human papillomavirus E6 proteins target the discs large tumour suppressor for proteasome-mediated degradation. Oncogene 18, 5487-5496.

Gewin, L., Galloway, D. A., 2001. E box-dependent activation of telomerase by human papillomavirus type 16 E6 does not require induction of c-myc. J. Virol. 75, 7198-7201.

Gewin, L., Myers, H., Kiyono, T., Galloway, D. A., 2004. Identification of a novel telomerase repressor that interacts with the human papillomavirus type-16 E6/E6-AP complex. Genes Dev. 18, 2269-2282.

Gry, M., Rimini, R., Strömberg, S., Asplund, A., Pontén, F., Uhlén, M., Nilsson, P., 2009. Correlations between RNA and protein expression profiles in 23 human cell lines. BMC Genomics 10, 365.

Hall, T. A., BioEdit: a user-friendly biological sequence alignment editor and analysis program for Windows 95/98/NT. Nucl. Acids Symp. Ser. 41, 95-98.

Hamilton, N., 2009. Quantification and its applications in fluorescent microscopy imaging. Traffic 10, 951-961.

Herráez, A., 2006. Biomolecules in the computer: Jmol to the rescue. Biochem. Mol. Biol. Educ. 34, 255-261.

Hofacker, I. L., 2003. Vienna RNA secondary structure server. Nucl. Acids Res. 31, 3429-3431.

Jackson, R., Togtema, M., Zehbe, I., 2013. Subcellular localization and quantitation of the human papillomavirus type 16 E6 oncoprotein through immunocytochemistry detection. Virology 435, 425-432.

Jiang, M., Milner, J., 2002. Selective silencing of viral gene expression in HPV-positive human cervical carcinoma cells treated with siRNA, a primer of RNA interference. Oncogene 21, 6041-6048.

Kaczkowski, B., Morevati, M., Rossing, M., Cilius, F., Norrild, B., 2012. A decade of global mRNA and miRNA profiling of HPV-positive cell lines and clinical specimens. Open Virol. J. 6, 216-231.

Katzenellenbogen, R. A., Egelkrout, E. M., Vliet-Gregg, P., Gewin, L. C., Gafken, P. R., Galloway, D. A., 2007. NFX1-123 and poly(A) binding proteins synergistically augment activation of telomerase in human papillomavirus type 16 E6-expressing cells. J. Virol. 81, 3786-3796.

Kauffmann, A. D., Campagna, R. J., Bartels, C. B., Childs-Disney, J. L., 2009. Improvement of RNA secondary structure prediction using RNase H cleavage and randomized oligonucleotides. Nucl. Acids Res. 37, e121.

Keel, A. Y., Rambo, R. P., Batey, R. T., Kieft, F. S., 2007. A general strategy to solve the phase problem in RNA crystallography.Structure 15, 761-772.

Kennedy, I. M., Haddow, J. K., Clements, J. B., 1991. A negative regulatory element in the human papillomavirus type 16 genome acts at the level of late mRNA stability. J. Virol. 65, 2093-2097.

Khairuddin, N., Gantier, M. P., Blake, S. J., Wu, S. Y., Behlke, M. A., Williams, B. R., McMillan, N. A., 2012. siRNA-induced immunostimulation through TLR7

promotes antitumoral activity against HPV-driven tumors in vivo. Immunol. Cell Biol. 90, 187-196.

Kiyono, T., Hiraiwa, A., Fujita, M., Hayashi, Y., Akiyama, T., Ishibashi, M., 1997. Binding of high-risk human papillomavirus E6 oncoproteins to the human homologue of the Drosophila discs large tumor suppressor protein. Proc. Natl. Acad. Sci. USA 94, 11612-11616.

Klingelhutz, A. J., Foster, S. A., McDougall, J. K., 1996. Telomerase activation by the E6 gene product of human papillomavirus type 16. Nature 380, 79-82.

Klingelhutz, A. J., Roman, A., 2012. Cellular transformation by human papillomaviruses: lessons learned by comparing high- and low-risk viruses. Virology 424, 77-98.

Koromilas, A. E., Li, S., Matlashewski, G., 2001. Control of interferon signaling in human papillomavirus infection. Cytokine Growth Factor Rev. 12, 157-170.

Kranjec, C. and Banks, L., 2011. A systematic analysis of human papillomavirus (HPV) E6 PDZ substrates identifies MAGI-1 as a major target of HPV type 16 (HPV-16) and HPV-18 whose loss accompanies disruption of tight junctions. J. Virol. 85, 1757-1764.

Krieger, E., Darden, T., Nabuurs, S. B., Finkelstein, A., Vriend, G., 2004. Making optimal use of empirical energy functions: force-field parameterization in crystal space. Proteins 57, 678-683.

Kretschmer-Kazemi Far, R., Sczakiel, G., 2003. The activity of siRNA in mammalian cells is related to structural target accessibility: a comparison with antisense oligonucleotides. Nucleic Acids Res. 31, 4417-4424.

Kumar, H., Kawai, T., Akira, S., 2011. Pathogen recognition by the innate immune system. Int. Rev. Immunol. 30, 16-34.

LaFleur, D. W., Nardelli, B., Tsareva, T., Mather, D., Feng, P., Semenuk, M., Taylor, K., Buergin, M., Chinchilla, D., Roshke, V., Chen, G., Ruben, S. M., Pitha, P. M., Coleman, T. A., Moore, P. A., 2001. Interferon-kappa, a novel type I interferon expressed in human keratinocytes. J. Biol. Chem. 276, 39765-39771.

Livak, K. J., Schmittgen, T. D., 2001. Analysis of relative gene expression data using real-time quantitative PCR and the 2(-delta delta c(t)) method. Methods 25, 402-408.

Mathews, D. H., 2006. Revolutions in RNA secondary structure prediction. J. Mol. Biol. 359, 526-532.

Meister, G., Landthaler, M., Patkaniowska, A., Dorsett, Y., Teng, G., Tuschl, T., 2004. Human Argonature2 mediates RNA cleavage targeted by miRNAs and siRNAs. Mol. Cell 15, 185-197.

Nakagawa, S., and Huibregtse, J. M., 2000. Human scribble (Vartul) is targeted for ubiquitin-mediated degradation by the high-risk papillomavirus E6 proteins and the E6AP ubiquitin-protein ligase. Mol. Cell Biol. 20, 8244-8253.

Nees, M., Geoghegan, J. M., Hyman, T., Frank, S., Miller, L., Woodworth, C. D., 2001. Papillomavirus type 16 oncogenes downregulate expression of interferon-responsive genes and upregulate proliferation-associated NF-kappaB-responsive genes in cervical keratinocytes. J. Virol. 75, 4283-4296.

Niccoli, S., Abraham, S., Richard, C., Zehbe, I., 2012. The Asian-American E6 variant protein of human papillomavirus 16 alone is sufficient to promote

immortalization, transformation, and migration of primary human foreskin keratinocytes. J. Virol. 86, 12384-12396.

Pante, N. and Kann, M., 2002. Nuclear pore complex is able to transport macromolecules with diameters of about 39 nm. Mol. Biol. Cell 13, 425-434.

Pattillo, R. A., Hussa, R. O., Story, M. T., Ruckert, A. C., Shalaby, M. R., Mattingly, R. F., 1977. Tumor antigen and human chorionic gonadotropin in CaSki cells: a new epidermoid cervical cancer cell line. Science 196, 1456-1458.

Pecot, C. V., Calin, G. A., Coleman, R. L., Lopez-Berestein, G., Sood, A. K., 2011. RNA interference in the clinic: challenges and future directions. Nat. Rev. Cancer 11, 59-67.

R Development Core Team, 2013. R: a language and environment for statistical computing. R Foundation for Statistical Computing, Vienna, Austria. ISBN 3-900051-074-0. Available at: http://www.R-project.org.

Reiser, J., Hurst, J., Voges, M., Krauss, P., Münch, P., Iftner, T., Stubenrauch, F., 2011. High-risk human papillomaviruses repress constitutive kappa interferon transcription via E6 to prevent pathogen recognition receptor and antiviral-gene expression. J. Virol. 85, 11372-11380.

Richard, C., Lanner, C., Naryzhny, S. N., Sherman, L., Lee, H., Lambert, P. F., Zehbe, I., 2010. The immortalizing and transforming ability of two common human papillomavirus 16 E6 variants with different prevalences in cervical cancer. Oncogene 29, 3435-3445.

Rincon-Orozco, B., Halec, G., Rosenberger, S., Muschik, D., Nindl, I., Bachmann, A., Ritter, T. M., Dondog, B., Ly, R., Bosch, F. X., Zawatzky, R., Rösl, F., 2009.

Epigenetic silencing of interferon-kappa in human papillomavirus type 16-positive cells. Cancer Res. 69, 8718-8725.

Ringnér, M., Krogh, M., 2005. Folding free energies of 5'-UTRs impact post-transcriptional regulation on a genomic scale in yeast. PLoS Comput. Biol. 1, e72.

Rivas, E., 2013. The four ingredients of single-sequence RNA secondary structure prediction: a unifying perspectice. RNA Biol. 10, Epub ahead of print.

Ronco, L. V., Karpova, A. Y., Vidal, M., Howley, P. M., 1998. Human papillomavirus 16 E6 oncoprotein binds to interferon regulatory factor-3 and inhibits its transcriptional activity. Genes Dev. 12, 2061-2072.

Sato K., Hamada, M., Asai, K., Mituyama, T., 2009. CENTROIDFOLD: a web server for RNA secondary structure prediction. Nucleic Acids Res. 37, W277-W280.

Scheffner, M. Huibregtse, J. M., Vierstra, R. D., Howley, P. M., 1993. The HPV-16 E6 and E6-AP complex functions as a ubiquitin-protein ligase in the ubiquitination of p53. Cell 75, 495-505.

Schneider-Gädicke, A., Schwarz, E., 1986. Different human cervical carcinoma cell lines show similar transcription patterns of human papillomavirus type 18 early genes. EMBO J. 5, 2285-2292.

Sekaric, P., Cherry, J. J., Androphy, E. J., 2008. Binding of human papillomavirus type 16 E6 to E6AP is not required for activation of hTERT. J. Virol. 82, 71-76.

Shapiro, B. A., Yingling, Y. G., Kasprzak, W., Bindewald, E., 2007. Bridging the gap in RNA structure prediction. Curr. Opin. Struct. Biol. 17, 157-165.

Sharma, S., Ding, F., Dokholyan, N. V., 2008. iFoldRNA: three-dimensional RNA structure prediction and folding. Bioinformatics 24, 1951-1952.

Shen, L. X., Basilion, J. P., Stanton Jr., V. P., 1999. Single-nucleotide polymorphisms can cause different structural folds of mRNA. Proc. Natl. Acad. Sci. USA 96, 7871-7876.

Shukla, S., Sumaria, C. S., Pradeepkumar, P. I., 2010. Exploring chemical modifications for siRNA therapeutics: a structural and functional outlook. ChemMedChem. 5, 328-349.

Singhania, R., Khairuddin, N., Clarke, D., McMillan, N. A., 2012. RNA interference for the treatment of papillomavirus disease. Open Virol. J. 6, 204-215.

Smotkin, D., Prokoph, H., Wettstein, F. O., 1989. Oncogenic and nononcogenic human genital papillomaviruses generate the E7 mRNA by different mechanisms. J. Virol. 63, 1441-1447.

Soldani, C., Scovassi, Al., 2002. Poly(ADP-ribose) polymerase-1 cleavage during apoptosis: an update. Apoptosis 7, 321-328.

Stern, P. L., van der Burg, S. H., Hampson, I. N., Broker, T. R., Fiander, A., Lacey, C. J., Kitchener, H. C., Einstein, M. H., 2012. Therapy of human-papillomavirus-related disease. Vaccine 30, F71-F82.

Tan, X., Lu, Z. J., Gao, G., Xu, Q., Hu, L., Fellmann, C., Li, M. Z., Qu, H., Lowe, S. W., Hannon, G. J., Elledge, S. J., 2012. Tiling genomes of pathogenic viruses identifies potent antiviral shRNAs and reveals a role for secondary structure in shRNA efficacy. Proc. Natl. Acad. Sci. USA 109, 869-874.

Thakur, N., Qureshi, A., Kumar, M., 2012. VIRsiRNAdb: a curated database of experimentally validated viral siRNA/shRNA. Nucleic Acids Res. 40, D230-236.

The 2008 Nobel Prize in Physiology or Medicine- Illustrated Presentation. Nobel Media AB. Available at: http://www.nobelprize.org/nobel_prizes/medicine/laureates/2008/illpres.html. Accessed 15 Jul 2013.

Thomas, M., Laura, R., Hepner, K., Guccione, E., Sawyers, C., Lasky, L., Banks, L., 2002. Oncogenic human papillomavirus E6 proteins target the MAGI-2 and MAGI-3 proteins for degradation. Oncogene 21, 5088-5096.

Togtema, M., Pichardo, S., Jackson, R., Lambert, P. F., Curiel, L., Zehbe, I., 2012. Sonoporation delivery of monoclonal antibodies against human papillomavirus 16 E6 restores p53 expression in transformed cervical keratinocytes. PLoS One 7, e50730.

Vaeteewoottacharn, K., Chamutpong, S., Ponglikitmongkol, M., Angeletti, P. C., 2005. Differential localization of HPV16 E6 splice products with E6-associated protein. Virol. J. 2, 50.

Van Doorslaer, K., Burk, R. D., 2012. Association between hTERT activation by HPV E6 proteins and oncogenic risk. Virology 433, 216-219.

Veldman, T., Liu, X., Yuan, H., Schlegel, R., 2003. Human papillomavirus E6 and Myc proteins associate in vivo and bind to and cooperatively activate the telomerase reverse transcriptase promoter. Proc. Natl. Acad. Sci. USA 100, 8211-8216.

Voinnet, O., 2005. Induction and suppression of RNA silencing: insights from viral infections. Nat. Rev. Genet. 6, 206-220.

Wang, Z., Gerstein, M., Snyder, M., 2009. RNA-Seq: a revolutionary tool for transcriptomics. Nat. Rev. Genet. 10, 57-63.

Wang, Z., Rao, D. D., Senzer, N., Nemunaitis, J., 2011.RNA interference and cancer therapy. Pharm. Res. 28, 2983-2995.

WHO/ICO Information Centre on HPV and Cervical Cancer (HPV Information Centre). Human papillomavirus and related cancers in world. Summary Report 2010. Available at: http://www.who.int/hpvcentre. Accessed 14 Jul 2013.

Woodman, C. B., Collins, S. I., Young, L.S., 2007. The natural history of cervical HPV infection: unresolved issues. Nat. Rev. Cancer 7, 11-22.

Yamada, T., Wheeler, C. M., Halpern, A. L., Stewart, A. C., Hildesheim, A., Jenison, S. A., 1995. Human papillomavirus type 16 variant lineages in United States populations characterized by nucleotide sequence analysis of the E6, L2, and L1 coding segments. J. Virol. 69, 7743-7753.

Yamato, K., Yamada, T., Kizaki, M., Ui-Tei, K., Natori, Y., Fujino M., Nishihara, T., Ikeda, Y., Nasu, Y., Saigo, K., Yoshinouchi, M., 2008. New highly potent and specific E6 and E7 siRNAs for treatment of HPV16 positive cervical cancer. Cancer Gene Ther. 15, 140-153.

Zanier, K., ould M'hamed ould Sidi, A., Boulade-Ladame, C., Rybin, V., Chappelle, A., Atkinson, A., Kieffer, B., Travé, G., 2012. Solution structure analysis of the HPV16 E6 oncoprotein reveals a self-association mechanism required for E6-mediated degradation of p53. Strucure 20, 604-617.

Zehbe, I., Moeller, H., Severini, A., Weaver, B., Escott, N., Bell, C., Crawford, S., Bannon, D., Paavola, N., 2011. Feasibility of self-sampling and human papillomavirus testing for cervical cancer screening in First Nation women from Northwest Ontario, Canada: a pilot study. BMJ Open 1, e000030.

Zehbe, I., Voglino, G., Delius, H., Wilander, E., Tommasino, M., 1998. Risk of cervical cancer and geographical variations of human papillomavirus 16 E6 polymorphisms. Lancet 352, 1441-1442.

Zhou J., Peng, C., Li, B., Wang, F., Zhou C., Hong, D., Ye, F., Cheng, X., Lü, W., Xie, X., 2012. Transcriptional gene silencing of HPV16 E6/E7 induces growth inhibition via apoptosis in vitro and in vivo. Gynecol. Oncol. 124, 296-302.

Zuker, M., 2003. Mfold web server for nucleic acid folding and hybridization prediction. Nucl. Acids Res. 31, 3406-3415.

zur Hausen, H., 1996. Papillomavirus infections-a major cause of human cancers. Biochim. Biophys. Acta 1288, F55-F78.

zur Hausen, H., 2002. Papillomaviruses and cancer: from basic studies to clinical application. Nat. Rev. Cancer 342, 342-350.

7 APPENDIX

7.1 E6 Knockdown Following Chemical Modification of the E6 siRNA with 2'-OMe Nucleotides

To determine whether greater E6 knockdown could be achieved through increasing siRNA stability and efficacy, the E6 siRNA sequence was modified through the addition of 2'-OMe bases (**Figure 18**) to the antisense strand in four patterns (**Table 4**). These patterns were chosen based on the findings of Dutta et al. (2011a and 2011b) which highlighted the importance of modifying these particular nucleotides. Chemical modifications at the 3' end are particularly important for improving exonuclease resistance (Dutta et al. 2011a).

The chemically modified sequences were also ordered from Sigma-Aldrich. AA E6 cells were chemically transfected with 10 nM of each of the four chemically modified E6 siRNA sequences, the unmodified sequence, or the scrambled control sequence and RT-qPCR was performed as described in Section 2.5.

Treatment with any of the E6 siRNA sequences resulted in significant decrease in E6 mRNA expression compared to the corresponding cells treated with scrambled siRNA ($P < 0.001$ for all) (**Figure 19**). However, none of the chemically modified sequences had significantly different knockdown efficacies compared to each other or the unmodified sequence.
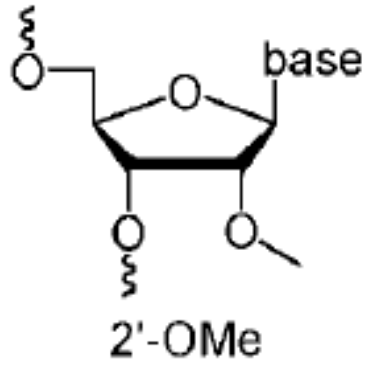
Figure 18. A 2'-OMe modified siRNA nucleotide. The hydroxyl group on the 2' carbon of the ribose ring is substituted for an OMe. Image taken from Shukla et al. 2010.

Table 4. 2'-OMe modified E6 siRNA sequences used in this study.

Sequence	Sense Strand	Anti-Sense Strand
E6 siRNA (Modification 1)	5' CCGUUGUGUGAUUUGUUAAU[dT] 3'	5' UUAACAAAUCACACAACGG**U**[dT] 3'*
E6 siRNA (Modification 2)	5' CCGUUGUGUGAUUUGUUAAU[dT] 3'	5' UUAACAAAUCAC**A**CAACGG**U**[dT] 3'*
E6 siRNA (Modification 3)	5' CCGUUGUGUGAUUUGUUAAU[dT] 3'	5' **U**UAACAAAUCACACAACGG**U**[dT] 3'*
E6 siRNA (Modification 4)	5' CCGUUGUGUGAUUUGUUAAU[dT] 3'	5' **U**UAACAAAUCAC**A**CAACGGU[dT] 3*'
E6 siRNA (Unmodified)	5' CCGUUGUGUGAUUUGUUAA[dT][dT] 3'	5' UUAACAAAUCACACAACGG[dT][dT] 3'
Srambled siRNA	5' UAUGUGCUAUGUAUUAUUG[dT][dT] 3'	5' CAAUAAUACAUAGCACAUA[dT][dT] 3'

*The first [dT] had to be changed to a U in the chemically modified sequences, as it was not possible to add a 2'-OMe to the DNA base. 2'-OMe bases are indicated in bold, underlined text.

HPV16 E6
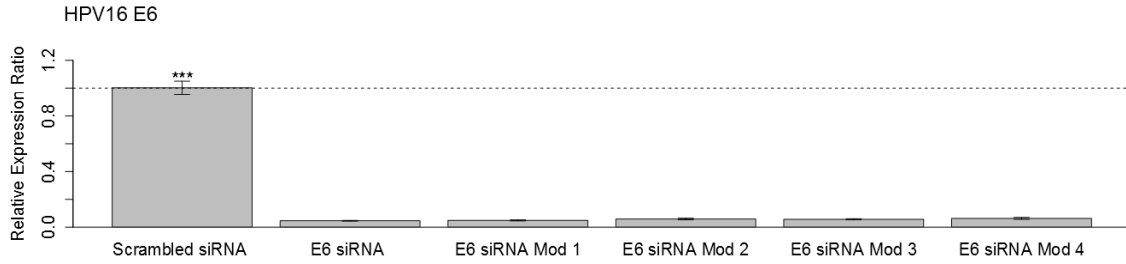
Figure 19. Relative E6 mRNA expression ratio in AA E6 cells following treatment with 10 nM 2'-OMe modified E6 siRNA. Treatment with any of the E6 siRNA sequences resulted in a significant decrease in E6 expression compared to cells treated with scrambled siRNA ($P < 0.001$ for all). None of the chemically modified siRNAs were more efficient than the others or compared to the unmodified siRNA. Expression was determined relative to HPRT1 and calibrated to cells treated with scrambled siRNA. Statistical analysis was performed using a one-way ANOVA followed by Tukey's HSD contrasts post hoc. Data represent mean ± SEM, $n = 3$ for all. *** denotes $P < 0.001$.